New indirect search for dark matter

Fa Peng Huang (黄发朋)
TianQin Center, SYSU

INPAC-TDLI Joint-Seminar@T.D. Lee Institute
March 30th, 2021

Outline

- ➢**Research Motivation**
- ➢**Indirect search for ultra-light dark matter(DM) by SKA-like experiments: axion DM, axion star, dark photon DM**
- ➢**Indirect search for heavy dark matter by phase transition gravitational wave**
- ➢**Conclusion**

Motivation

Whenever we see this cosmic pie, we are always confused: what is the nature of DM? Many experiments have been done to unravel this long-standing problem. However, there are no expected signals at LHC and DM direct search.

This situation may point us towards new approaches, such as
the Radio telescope experiments (SKA, FAST, GBT…)
the Laser Interferometer experiments (TianQin/LISA…)

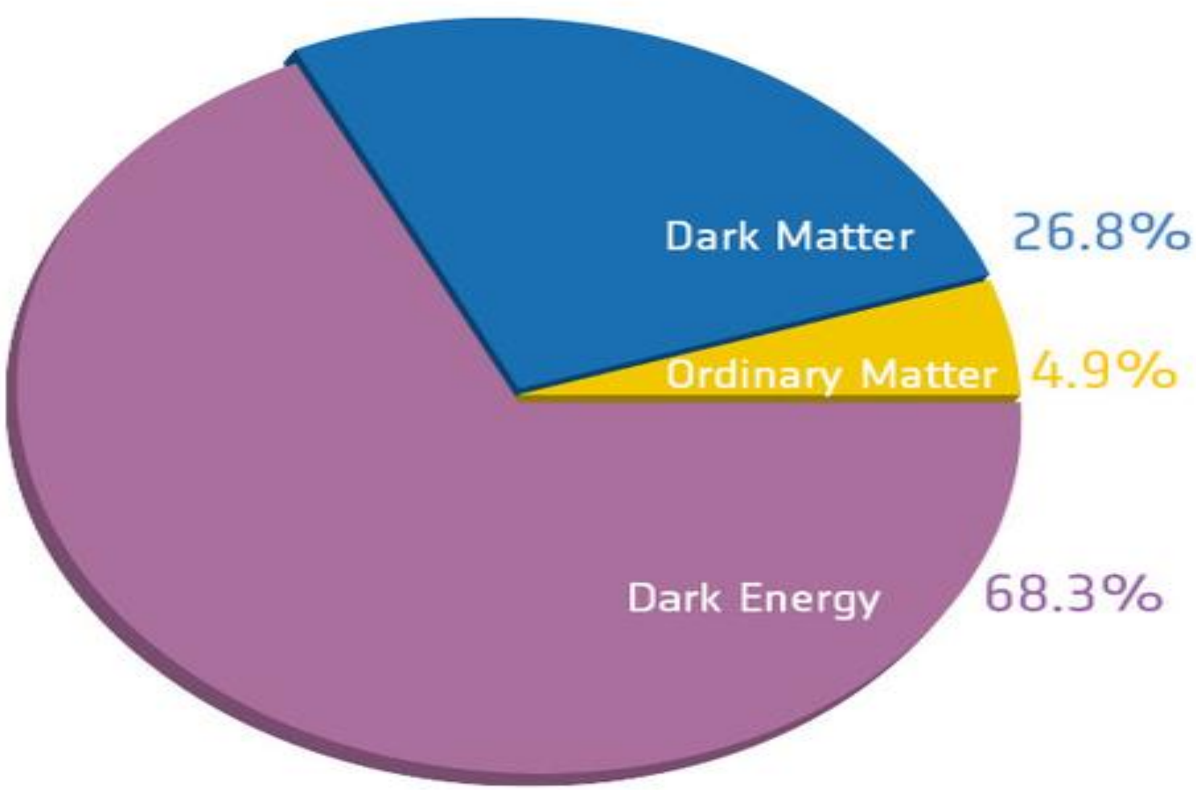

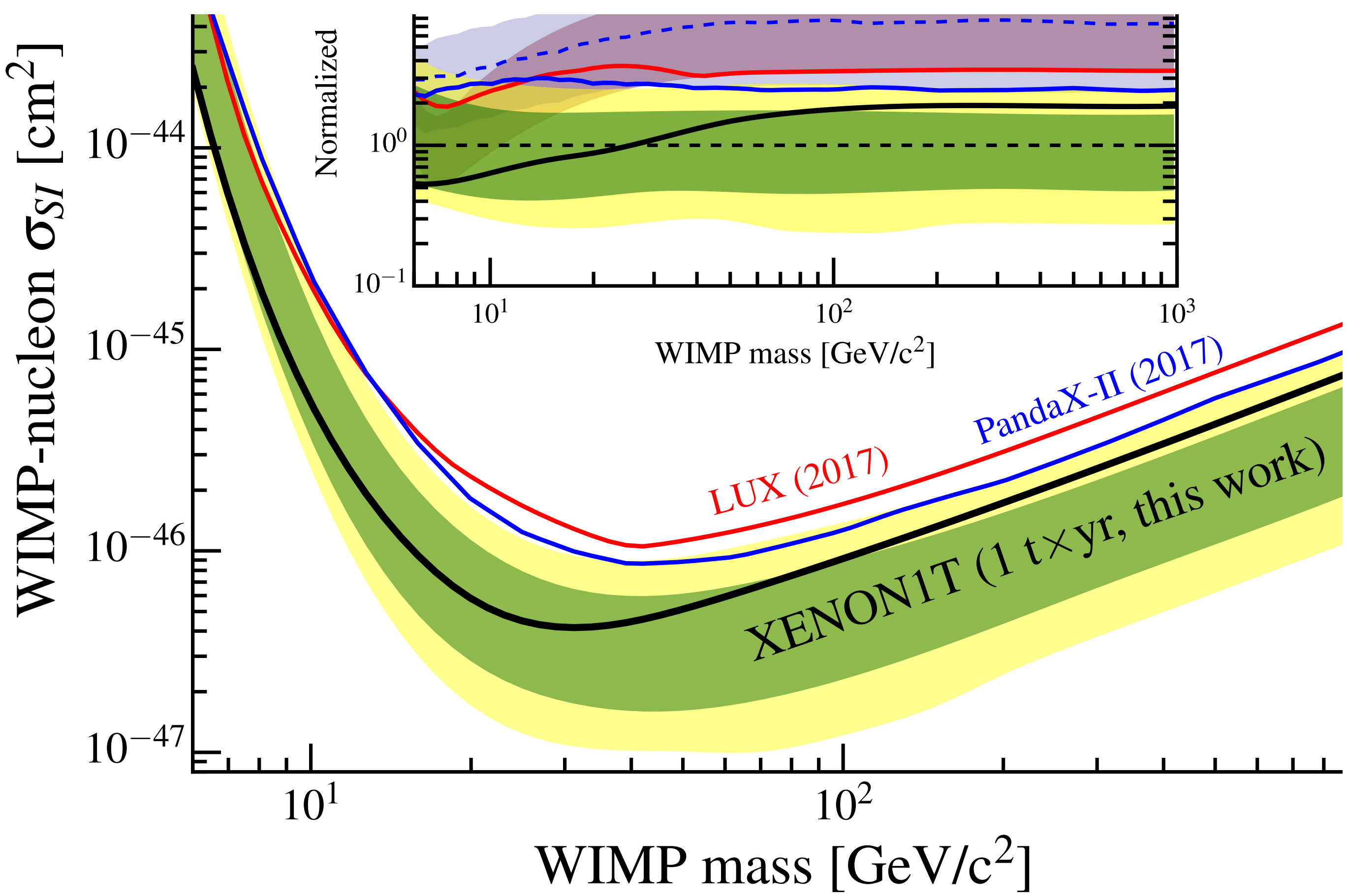

Phys.Rev.Lett. 121 (2018) no.11, 111302

What is dark matter?

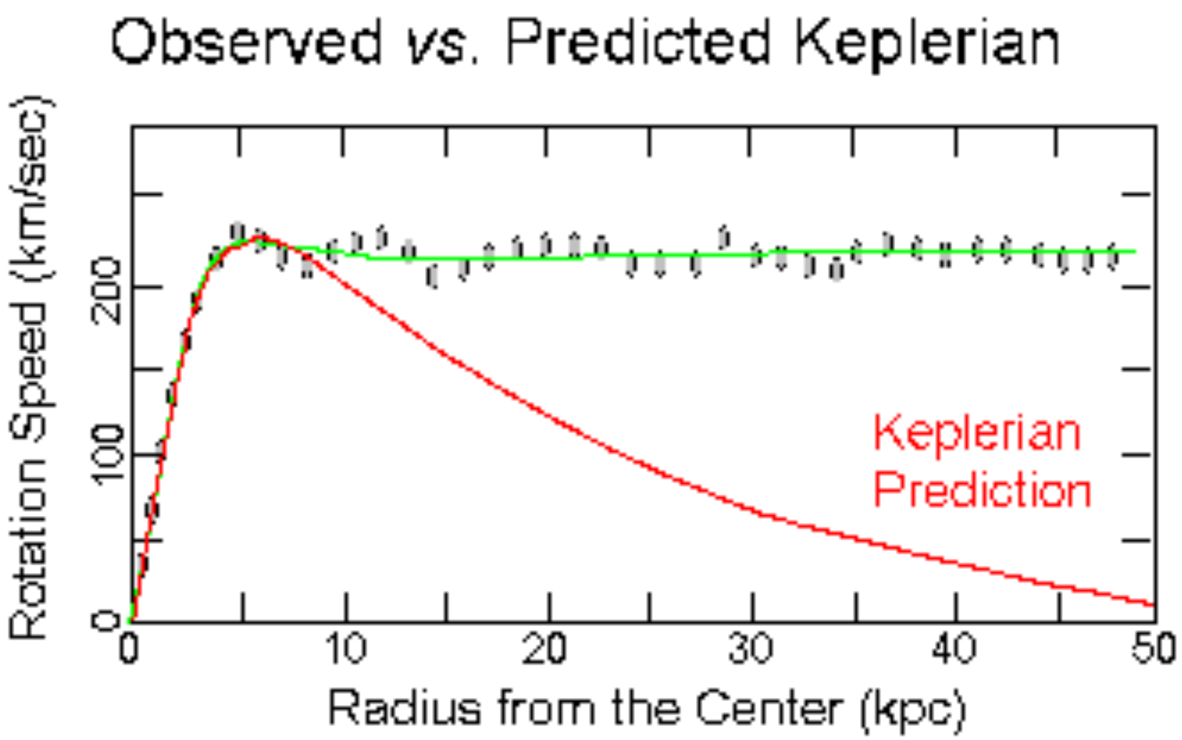

Galaxy rotation curve

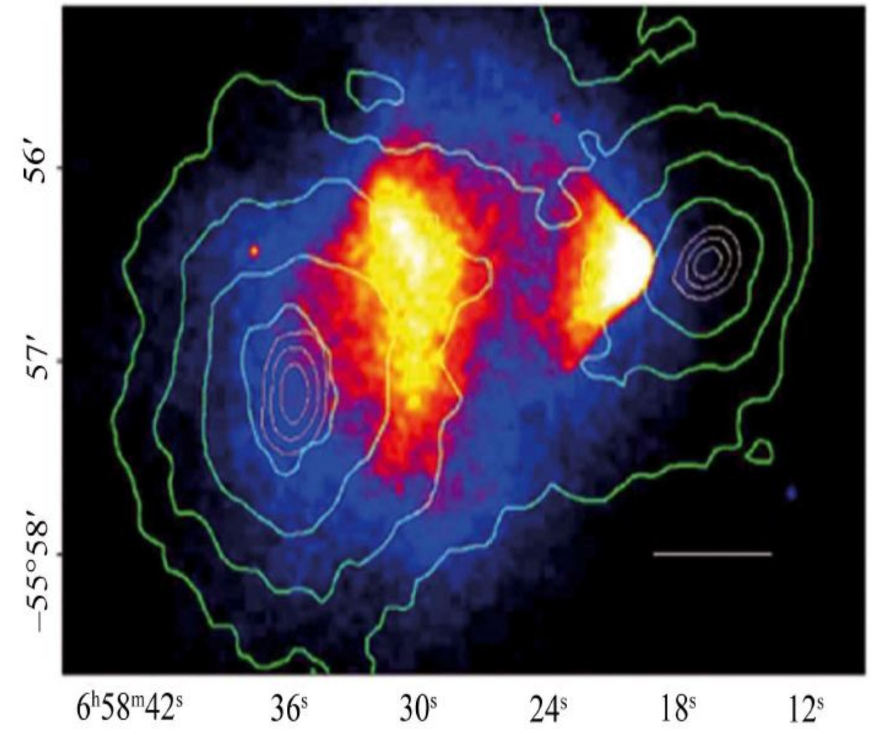

Bullet cluster collision

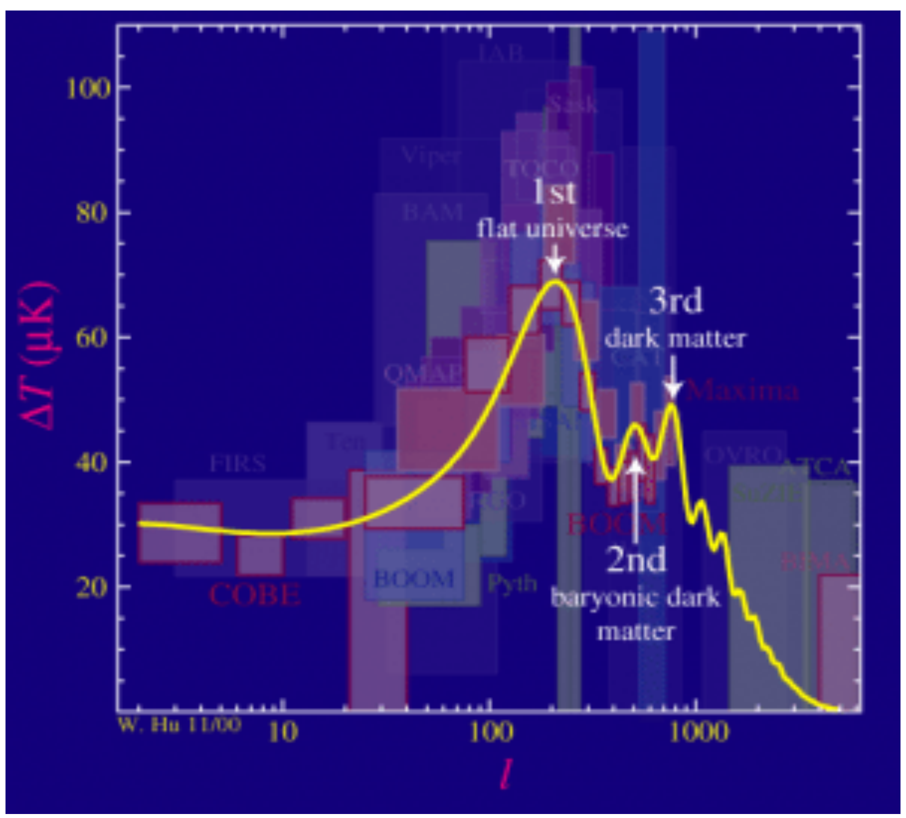

CMB spectrum

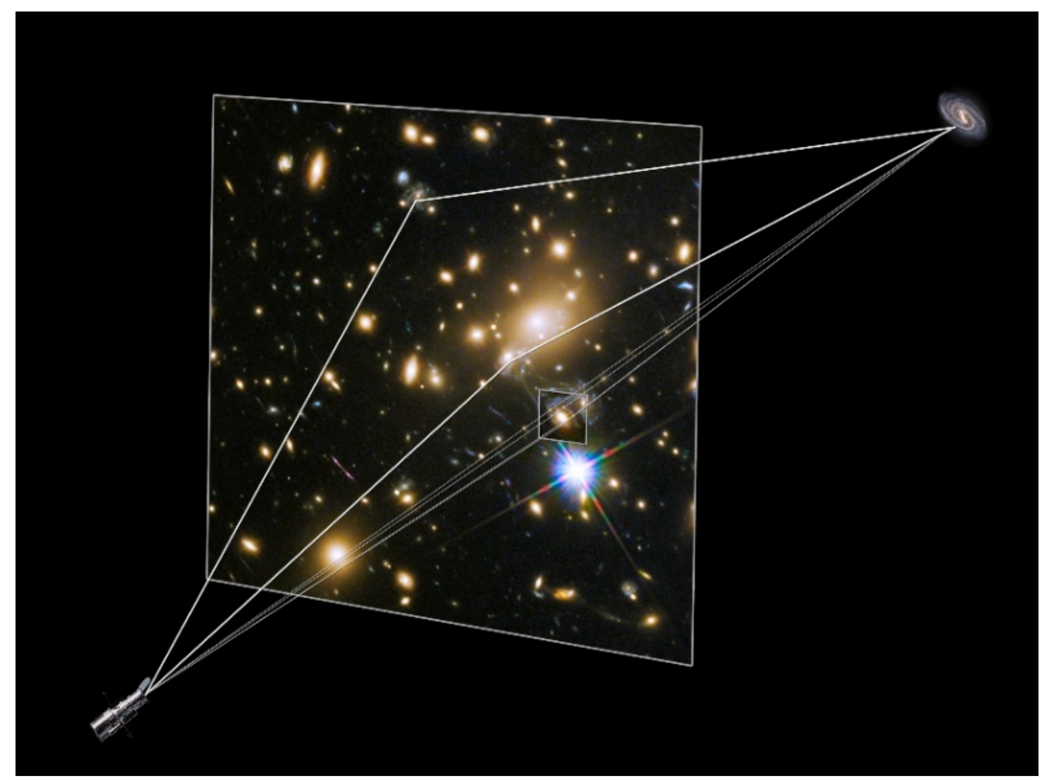

Gravitational lensing

Motivation

EW phase transition and baryogenesis: LISA, Tianqin/Taiji

QCD phase transition and axion cold dark matter: SKA, FAST, GBT(radio telescope)

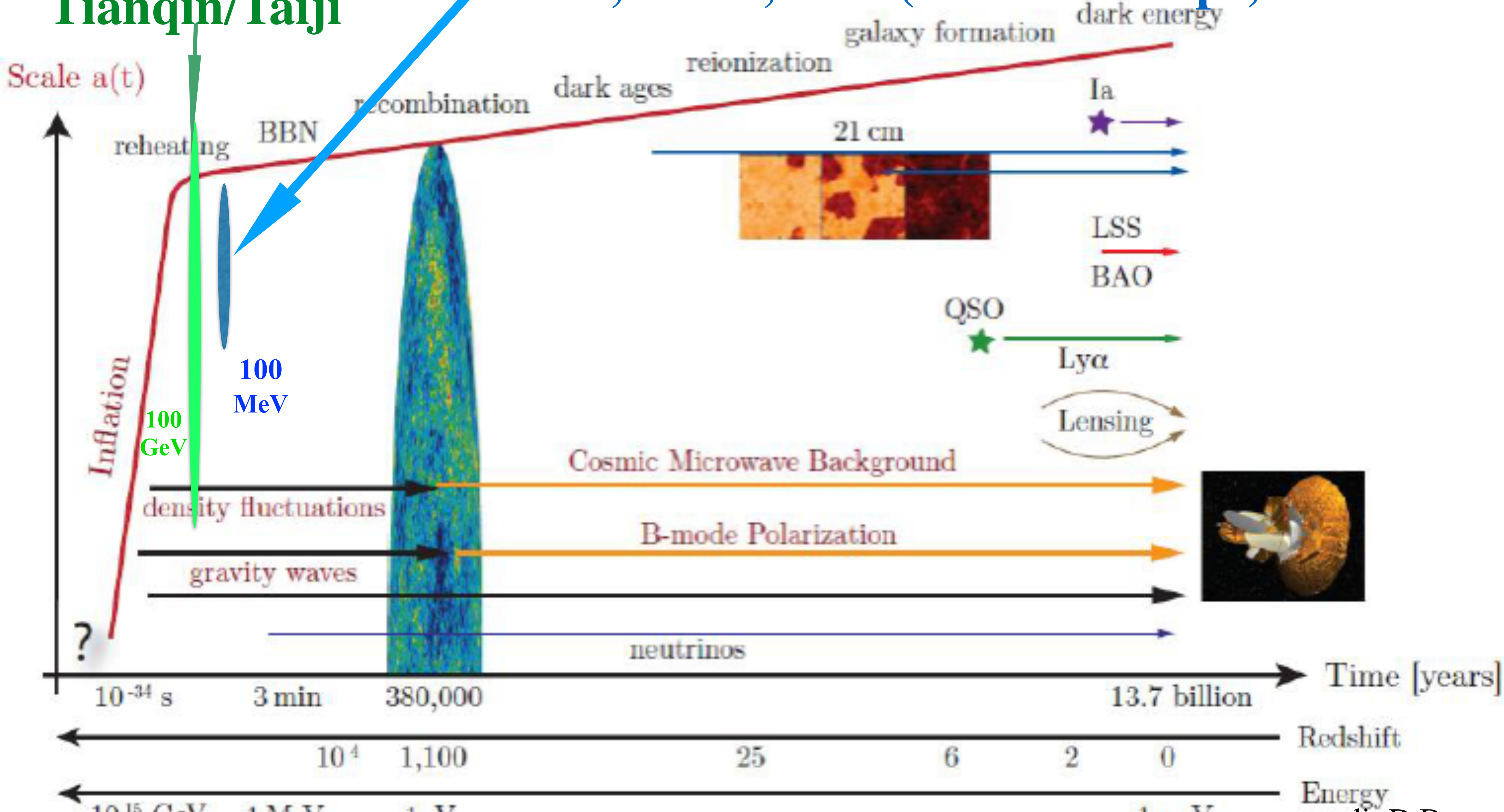

credit:D.Baumann

Ⅰ.Explore diffused dark matter by SKA

Axion or axion-like particle motivated from strong CP problem or string theory is still one of the most attractive and promising dark matter candidate.

We firstly study using the SKA-like experiments to explore the resonant conversion of axion cold dark matter to radio signal from magnetized astrophysical sources, such as neutron star, magnetar and pulsar.

FPH, K. Kadota, T. Sekiguchi, H. Tashiro, Phys.Rev. D97 (2018) no.12, 123001, arXiv:1803.08230

The Square Kilometre Array (SKA)

Early science observations are expected to start in 2021 with a partial array.

credit: SKA website

The Five-hundred-meter Aperture Spherical radio Telescope (FAST)

From 25 Sep. 2016

Credit:FAST website

The Green Bank Telescope (GBT)

GBT is running observations roughly 6,500 hours each year

credit:GBT website

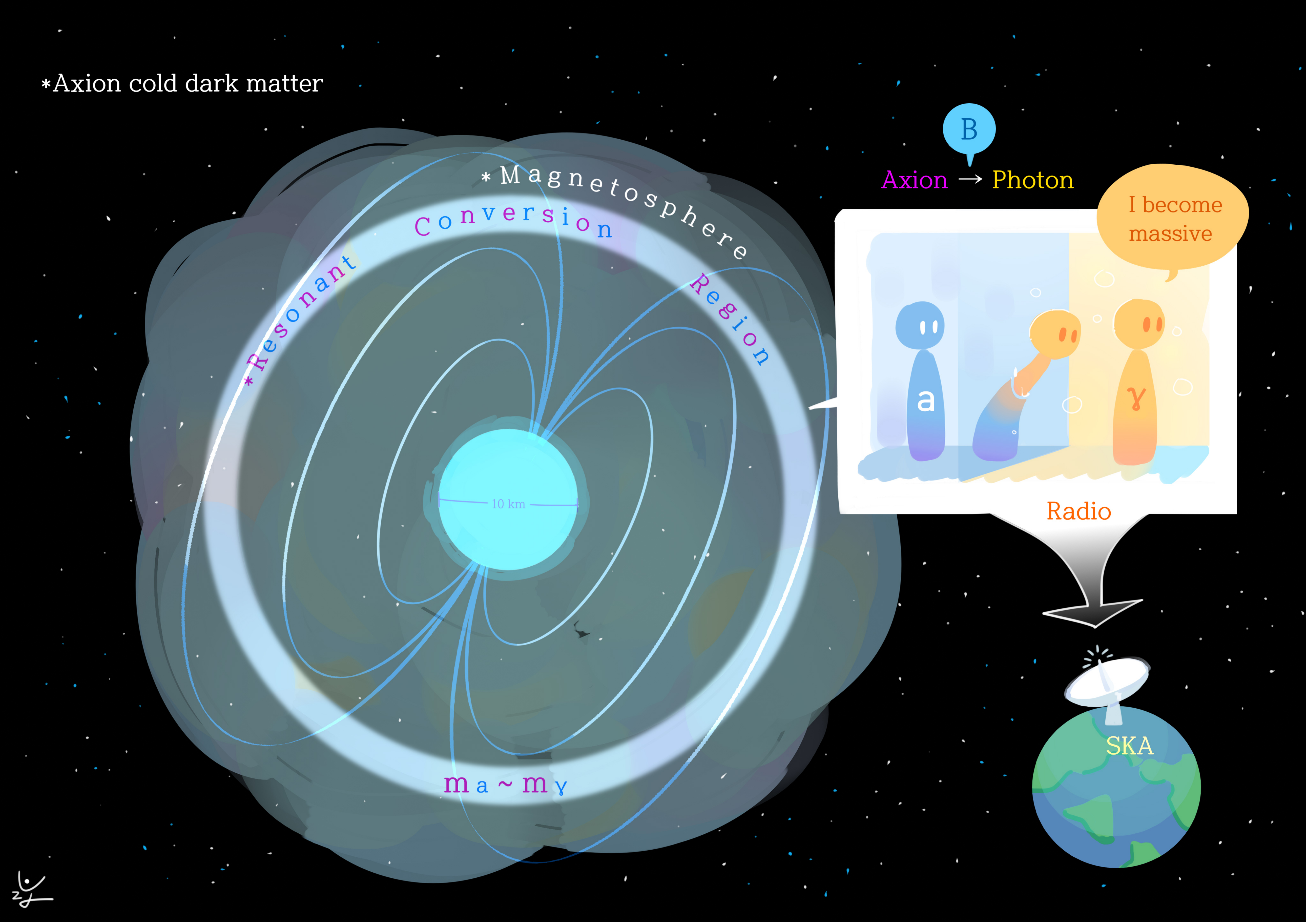

FPH, **K. Kadota, T. Sekiguchi, H. Tashiro, Phys.Rev. D97 (2018) no.12, 123001**

Radio telescope search for the resonant conversion of cold dark matter axions from the magnetized astrophysical sources

Three key points:

- ➢Cold DM is composed of non-relativistic axion or axion-like particles, and can be accreted around the neutron star
- ➢Neutron star (or pulsar and magnetar) has the strongest position-dependent magnetic field in the universe
- ➢Neutron star is covered by magnetosphere and photon becomes massive in the magnetosphere

Quick sketch of the neutron star size

The radius of the neutron star is slightly larger than the radius of the LHC circle.

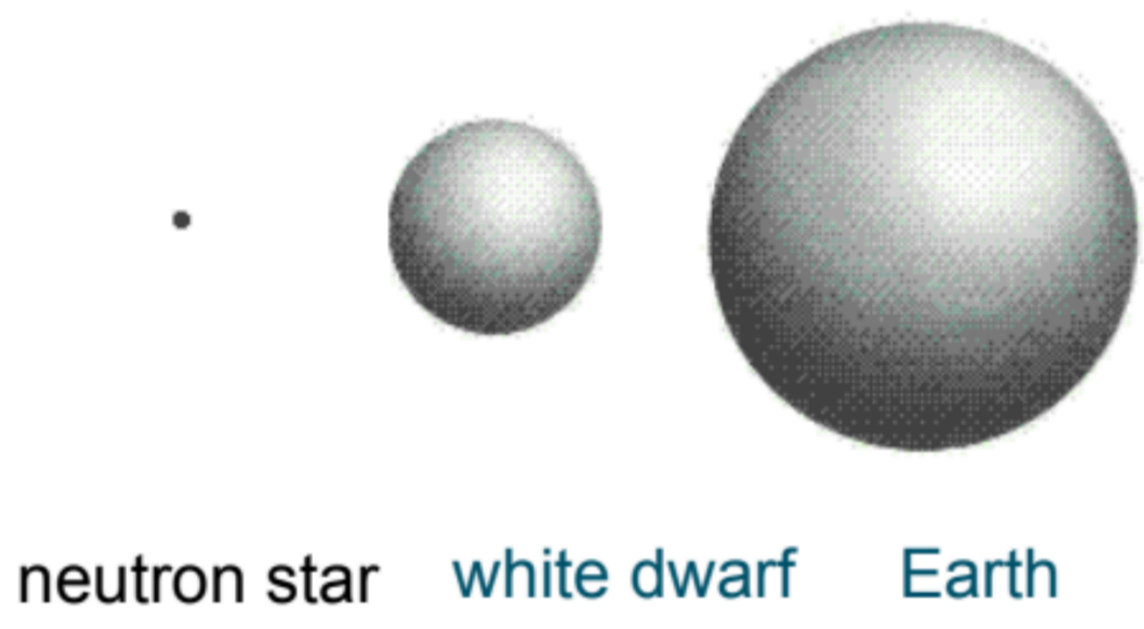

Strong magnetic field in the magnetosphere of Neutron star, Pulsar, Magnetar: the strongest magnetic field in the universe

1. **Mass:from 1 to 2 solar mass**

2. **Radius:** $r_0 \sim 10 - 20\text{km}$

The typical diameter of neutron star is just half Marathon.

3. **Strongest magnetic field at the surface of the neutron star**

$$B_0 \approx 10^{12} - 10^{15}\text{G}$$

$$B_0 \sim 3.3 \times 10^{19} \sqrt{P\dot{P}} \quad \text{G}$$

P is the period of neutron star

4. **Neutron star is surrounded by large region of magnetosphere, where photon becomes massive.**

Alfven $r \sim 100 r_0$

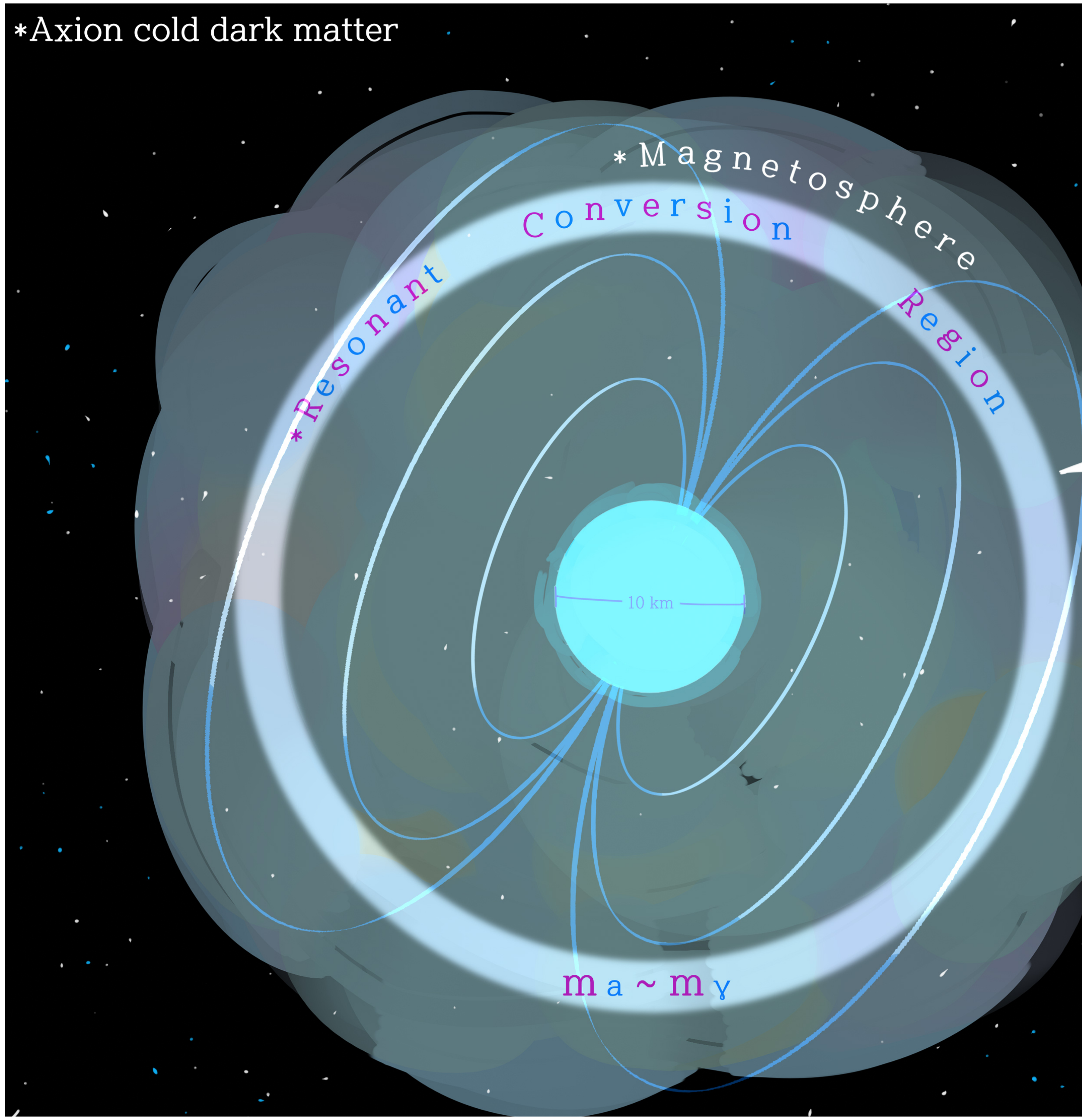

Axion-photon conversion in the magnetosphere

$$L_{\text{int}} = \frac{1}{4} g \tilde{F}^{\mu\nu} F_{\mu\nu} a = -g \mathbf{E} \cdot \mathbf{B} a,$$

Massive Photon: In the magnetosphere of the neutron star, photon obtains the effective mass in the magnetized plasma. $m_\gamma^2 = \omega_{plasma}^2 = 4\pi\alpha \frac{n_e}{m_e}$

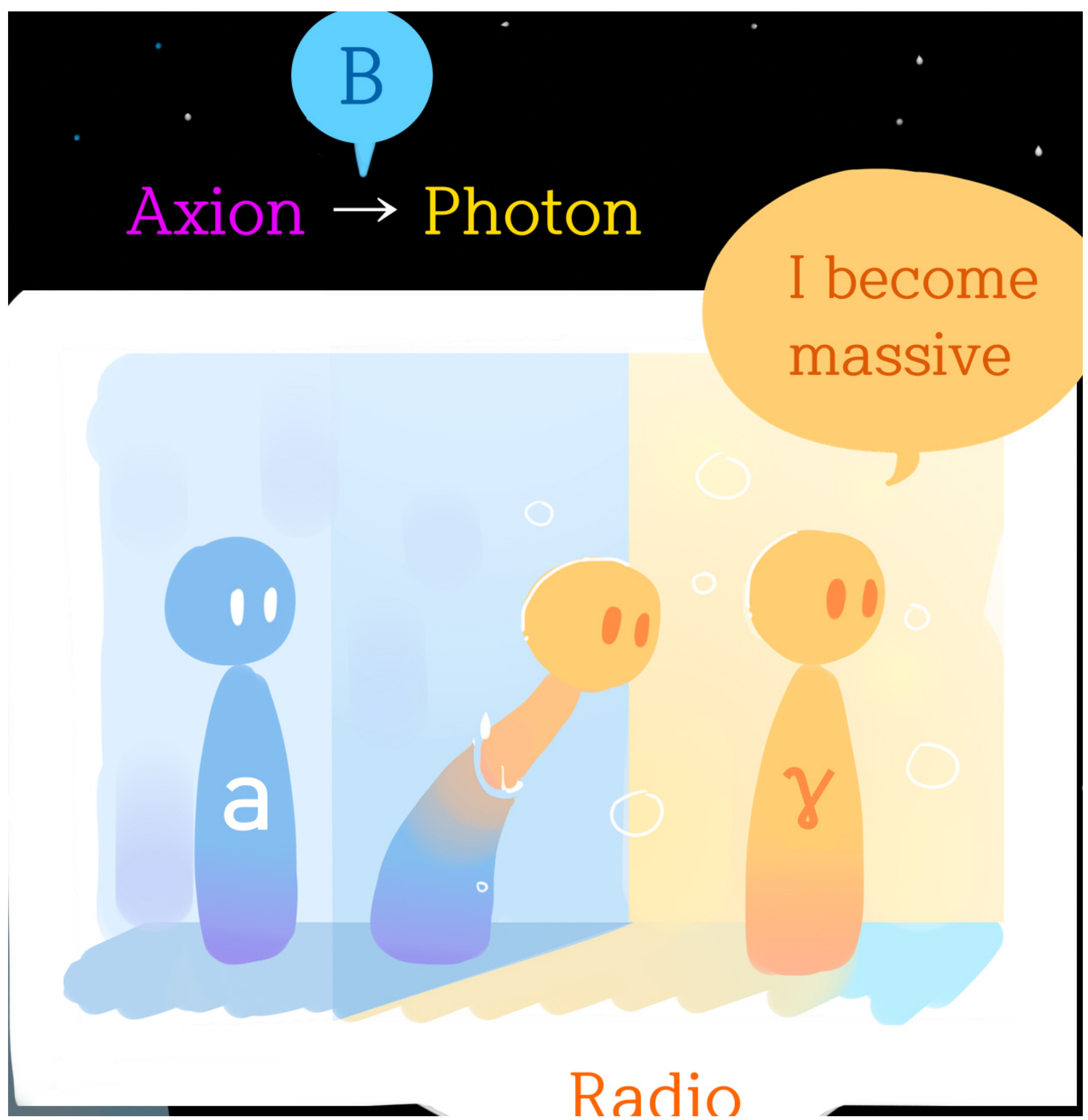

Axion-photon conversion in magnetosphere

Here, we choose the simplest magnetic field configuration and electron density distribution to clearly see the underlying physics.

$$m_\gamma^2(r) = 4\pi\alpha \frac{n_e(r)}{m_e} \qquad B(r) = B_0 \left(\frac{r}{r_0}\right)^{-3}$$

$$n_e(r) = n_e^{\mathrm{GJ}}(r) = 7 \times 10^{-2} \frac{1s}{P} \frac{B(r)}{1\ \mathrm{G}} \frac{1}{\mathrm{cm}^3}$$

Thus, the photon mass is position r dependent, and within some region the photon mass is close to the axion DM mass.

The Adiabatic Resonant Conversion

$$m_\gamma^2(r_{\rm res}) = m_a^2$$

The resonance radius is defined at the level crossing point

At the resonance, $|m_\gamma^2 - m_a^2| \ll gB\omega$ and $m_{1,2}^2 \approx m_a^2 \pm gB\omega$.

Within the resonance region, the axion-photon conversion rate is greatly enhanced due to large mixing angle.

The adiabatic resonant conversion requires the resonance region is approximately valid inside the resonance width. Coherent condition is also needed.

Resonant conversion is essential to observe the radio signal.

Radio Signal

Line-like radio signal for non-relativistic axion conversion:

$$\nu_{\rm peak} \approx \frac{m_a}{2\pi} \approx 240 \frac{m_a}{\mu eV} {\rm MHz}$$

1 GHz ~ 4 μeV

The FAST covers 70 MHz–3 GHz, the SKA covers 50 MHz–14 GHz, and the GBT covers 0.3–100 GHz, so that the radio telescopes can probe axion mass range of 0.2–400 μeV

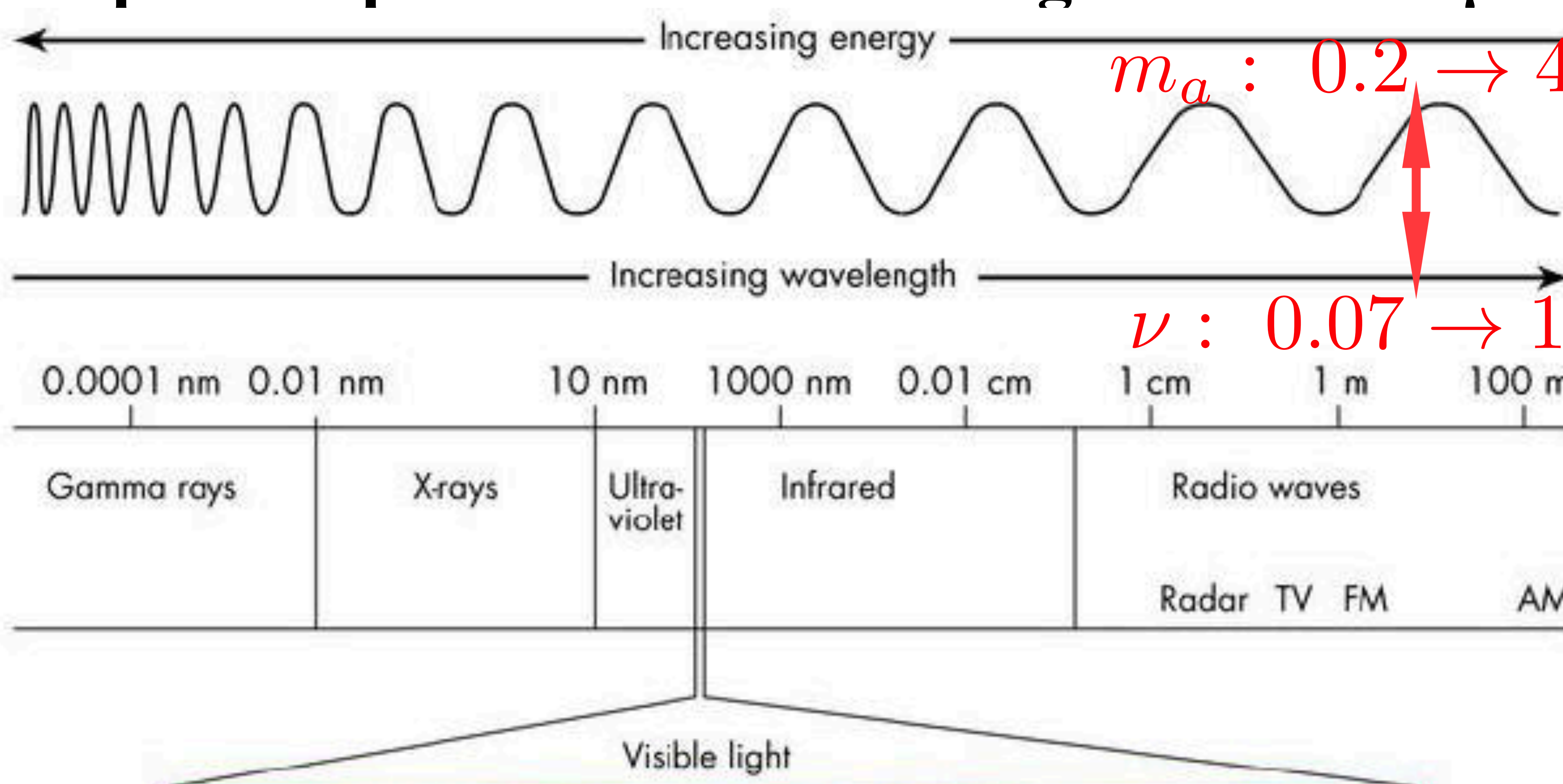

$m_a: \ 0.2 \rightarrow 400 \ \mu{\rm eV}$

$\nu: \ 0.07 \rightarrow 100 \ {\rm GHz}$

Radio Signal

Signal: For adiabatic resonant conversion, and the photon flux density can be estimated to be of order

$$S_\gamma = \frac{dE/dt}{4\pi d^2 \Delta\nu} \sim 4.2\mu Jy \frac{\left(\frac{r_{\rm res}}{100\ {\rm km}}\right)\left(\frac{M}{M_{\rm sun}}\right)\left(\frac{\rho_a}{0.3\ {\rm GeV/cm^3}}\right)\left(\frac{10^{-3}}{v_0}\right)\left(\frac{g}{1/10^{10}\ {\rm GeV}}\right)\left(\frac{B(r_{\rm res})}{10^{12}\ {\rm G}}\right)\left(\frac{\omega}{\mu{\rm eV}}\right)\left(\frac{\mu{\rm eV}}{m_a}\right)^2}{\left(\frac{d}{1\ {\rm kpc}}\right)^2\left(\frac{m_a/2\pi}{\mu{\rm eV}/2\pi}\right)\left(\frac{v_{\rm dis}}{10^{-3}}\right)},$$

where d represents the distance from the neutron star to us. The photon flux peaks around the frequency $\nu_{\rm peak} \sim m_a/2\pi$, and $\Delta\nu \sim \nu_{\rm peak} v_{\rm dis}$ represents the spectral line broadening around this peak frequency due to the DM velocity dispersion $v_{\rm dis}$.

Sensitivity: The smallest detectable flux density of the radio telescope (SKA, FAST, GBT) is of order

$$S_{\rm min} \approx 0.29\mu Jy \left(\frac{1\ {\rm GHz}}{\Delta B}\right)^{1/2}\left(\frac{24\ {\rm hrs}}{t_{\rm obs}}\right)^{1/2}\left(\frac{10^3\ {\rm m^2/K}}{A_{\rm eff}/T_{\rm sys}}\right)$$

Radio Signal

Signal: For a trial parameter set, $B_0 = 10^{15}$ G, $m_a = 50\ \mu$eV
$P = 10$ s, $g = 5 \times 10^{-11}$ GeV^{-1}, $r_0 = 10$ km, $M = 1.5 M_{\rm sun}$, $d = 1$kpc
satisfies the conditions for the adiabatic resonance conditions and the existed axion search constraints with signal $S_\gamma \sim 0.51\ \mu$Jy.

Sensitivity: $S_{\rm min} \sim 0.48 \mu Jy$ for the SKA1

$S_{min} \sim 0.016 \mu Jy$ for SKA2 with 100 hours observation time.

SKA-like experiment can probe the axion dark matter and the axion mass which corresponds to peak frequency.
More detailed study taking into account astrophysical uncertainties and more quantitatively numerical analysis for our adiabatic resonance conversion scenario is still working in progress.

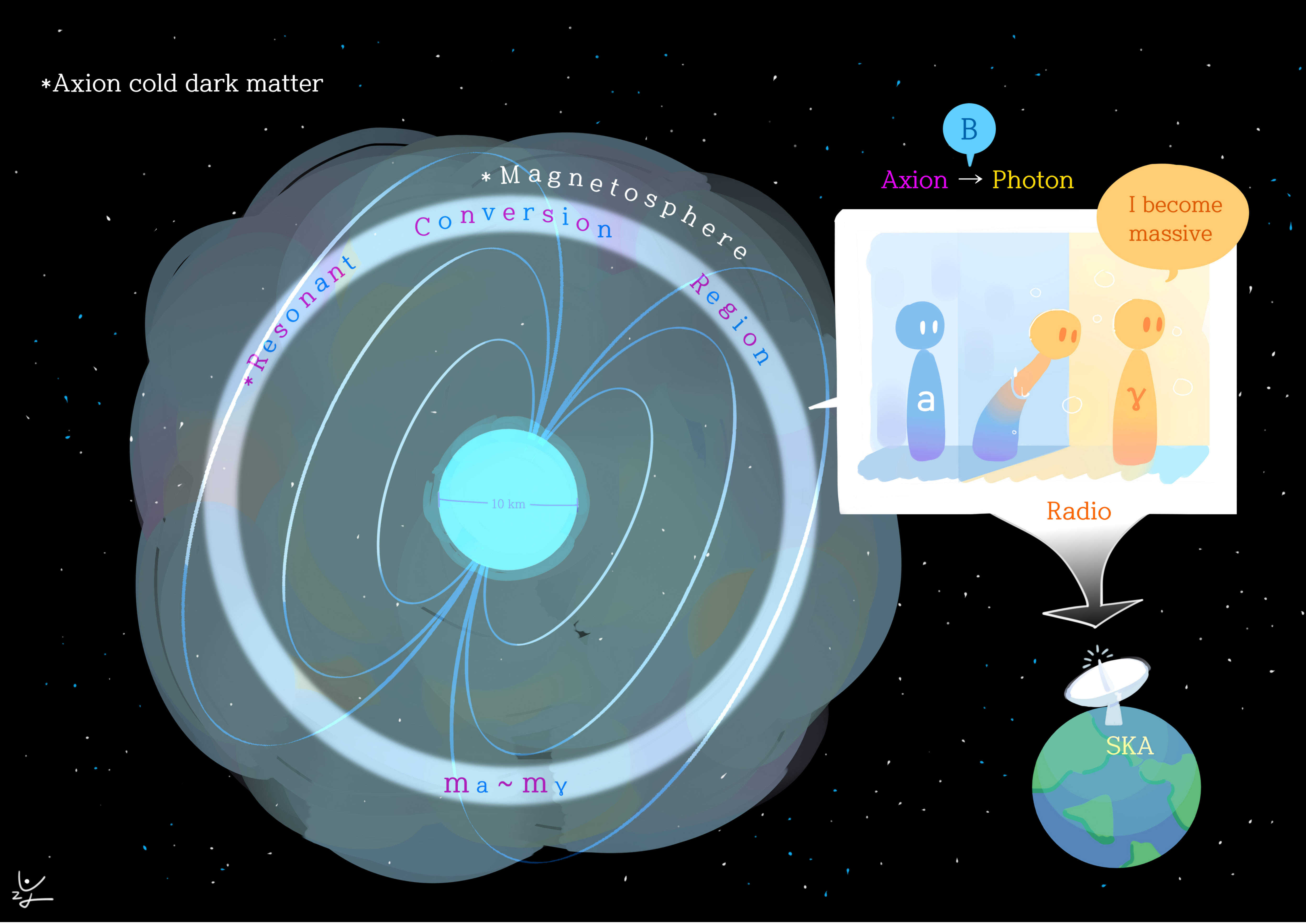

FPH, K. Kadota, T. Sekiguchi, H. Tashiro, Phys.Rev. D97 (2018) no.12, 123001

Comments on the radio probe of axion dark matter

1. Astrophysical uncertainties:the magnetic profile of the neutron star, the dark matter density around the neutron star, the location of the neutron star, the velocity dispersion, the plasma mass, background including the optimized bandwidth…

2. There are more and more detailed studies after our first estimation on the radio signal:

arXiv:1804.03145 by Anson Hook, Yonatan Kahn, Benjamin R. Safdi, Zhiquan Sun where they consider more details and extremely high dark matter density around the neutron star, thus the signal is more stronger.

arXiv:1811.01020 by Benjamin R. Safdi, Zhiquan Sun, Alexander Y. Chen

arXiv:1905.04686,Thomas, D.P.Edwards,Marco Chianese, Bradley J. Kavanagh, Samaya M. Nissanke, Christoph Weniger, where they consider multi-messenger of axion dark matter detection. Namely, using LISA to detect the dark matter density around the neutron star, which can determine the radio strength detected by SKA

This idea becomes a hot topic.

FPH, K. Kadota, T. Sekiguchi, H. Tashiro, Phys.Rev. D97 (2018) no.12, 123001, arXiv:1803.08230, Cited by 39 times, including nature and PRL papers.

Invisible Axion Search Methods

Pierre Sikivie (Florida U.) (Mar 4, 2020)

Published in: *Rev.Mod.Phys.* 93 (2021) 1, 015004 • e-Print: 2003.02206 [hep-ph]

Axion-photon conversion can occur in astrophysical magnetic fields, and may have implications for observation. Axions can readily convert to photons, and vice-versa, in the magnetospheres of neutron stars (Hook *et al.*, 2018; Huang *et al.*, 2018; Morris, 1986). With

Physics Briefing Book : Input for the European Strategy for Particle Physics Update 2020

Richard Keith Ellis (Durham U., IPPP) *et al.*. Oct 25, 2019. 254 pp.

CERN-ESU-004

e-Print: arXiv:1910.11775 [

9.5.3 Complementarity with direct and indirect detection searches

Radio searches for the conversion of axion/ALP dark matter into photons inside the magnetosphere of neutron stars can have sensitivity [630–632] for ALP masses in the range ~ 0.2–$40\,\mu$eV, and potentially above. The signature is the emission of a narrow radio line from individual neutron stars, with a frequency that corresponds to the mass of the ALP. Several of such searches are now underway, with expected sensitivities to the photon-ALP coupling down to $g_{a\gamma\gamma} \sim 10^{-12}\,\mathrm{GeV}^{-1}$. The future SKA may have the ability to probe significant parts of the QCD axion parameter space [633].

Generalization to axion star case

Axion DM can condense to BEC and then form axion star. We study the radio signal of dense axion star and use it to explain the FRBs.

James Buckley, Bhupal Dev, Francesc Ferrer, FPH,
arXiv:2004.06486, *Phys.Rev.D* 103 (2021) 4, 043015,
Fast radio bursts from axion stars moving through pulsar magnetospheres

arXiv:2102.05680, Sami Nurmi, Enrico D. Schiappacasse, and Tsutomu T. Yanagida

FRB-Axion star correlation

A collection of axions can condense into a bound Bose-Einstein condensate called an axion star. The typical axion star mass is $10^{-13} M_{\odot}$

The fact that the energy released by FRBs is close to $10^{-13} M_{\odot}$ **, which is the typical axion star mass, and that their frequency (several hundred MHz to several GHz) coincides with that expected from** μ**eV axion particles, motivates us to further explore whether the axion-FRB connection can be made viable in a pulsar magnetosphere and tested with the future data.**

Axion star-Neutron star encounter

Dilute axion star is balanced by kinetic pressure and self-gravity, with the following radius

$$R_a^{\rm dilute} \sim \frac{1}{G_N M_a m_a^2} \cong 270 \left(\frac{10\ \mu{\rm eV}}{m_a}\right)^2 \left(\frac{10^{-12} M_\odot}{M_a}\right)\ {\rm km}$$

In this work, we assume that dense axion stars with a mass around $10^{-13} M_\odot$ can survive to the present, and have a chance to encounter a neutron star for some very flat axion potential. The radius of a dense axion star is

$$R_a^{\rm dense} \sim 0.47\sqrt{g_{a\gamma\gamma} \times 10^{13}\ {\rm GeV}} \times \sqrt{\frac{10\ \mu{\rm eV}}{m_a}} \left(\frac{M_a}{10^{-13} M_\odot}\right)^{0.3}\ {\rm m}$$

Tidal effects

A gravitationally bound object approaching a star closer than Roche limit will be disrupted by tidal effects. The Roche limit is

$$r_t = R_a \left(\frac{2M_{\rm NS}}{M_a} \right)^{1/3}$$

Tidal disruption may quickly rip apart the dilute axion star, producing a stream of axion debris, long before a dilute axion star enters the magnetosphere of neutron star. For100 km dilute axion, the Roche limit is about 10^6 km.

For a dense axion star, the radius is smaller than 1m and the Roche limit is below 10 km. Thus, a dense axion star can reach the resonant conversion region without being tidally ripped.

tidal deformation ratio

$$\frac{\delta R_a}{R_a} = \frac{9M_{\rm NS}}{8\pi\rho_{\rm AS} r^3}$$

Mysterious FRBs

In recent ten years, Fast Radio Bursts (FRBs) become the most mysterious phenomenon in astrophysics and cosmology, especially from 2013(D. Thornton, et al., (2013) Science, 341, 53). They are intense, transient radio signals with large dispersion measure, light years away. However, their origin and physical nature are still obscure.

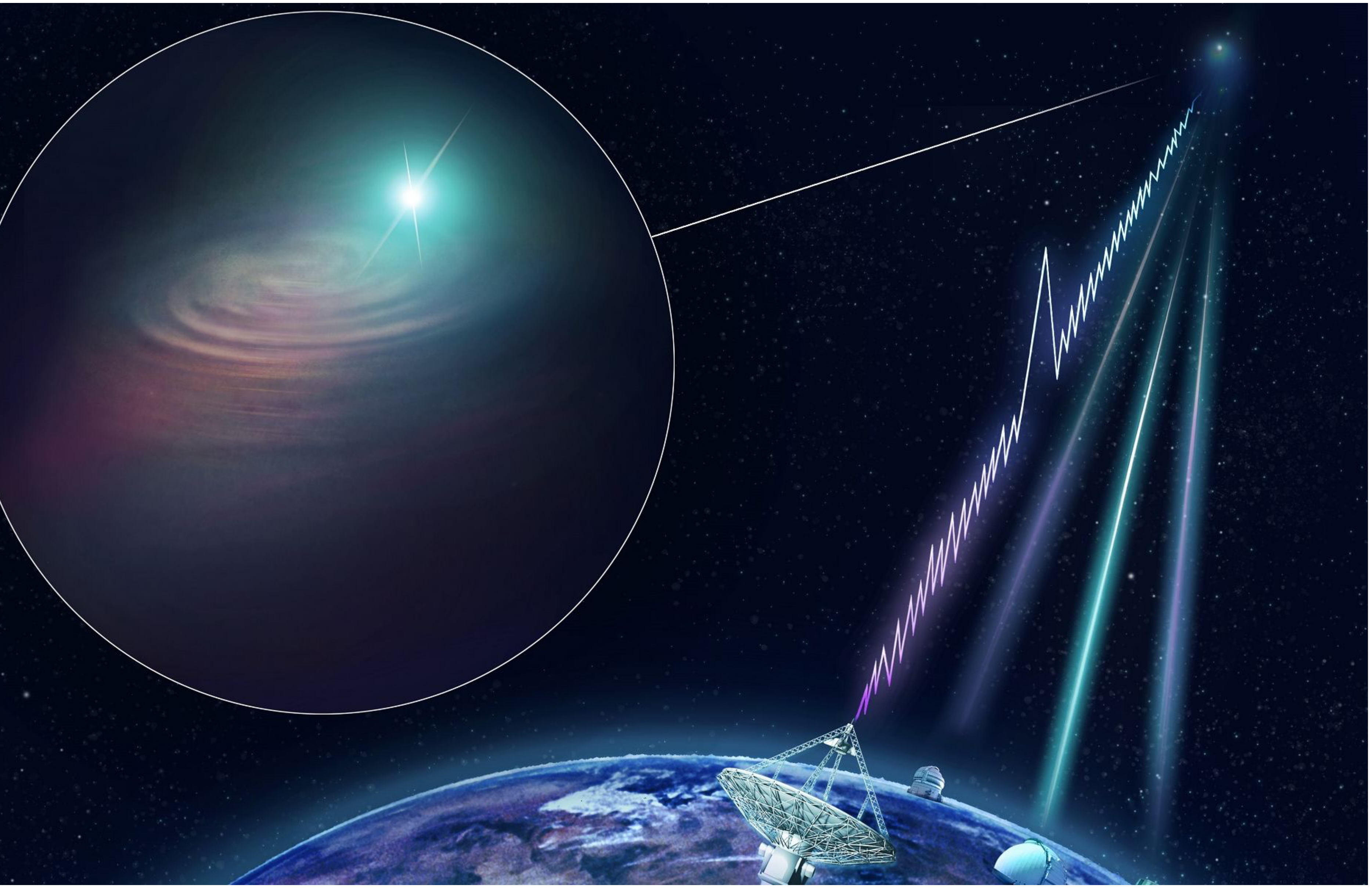

$\mathcal{O}(0.1)$ to $\mathcal{O}(100)$ Jy

$\mathcal{O}(10^{38})$ to $\mathcal{O}(10^{40})$ erg

Duration: milliseconds

$$0.1 \lesssim z \lesssim 2.2$$

We focus on FRBs events with frequency range 800 MHz to 1.4GHz mainly observed by Parkes, ASKAP, and UTMOST.

We do not include other non-repeating FRBs with frequencies lower than 800 MHz, like the events from CHIME and Pushchino, which may be better explained by a lighter axion or other sources.

From Universe Today

FRB-Axion star correlation

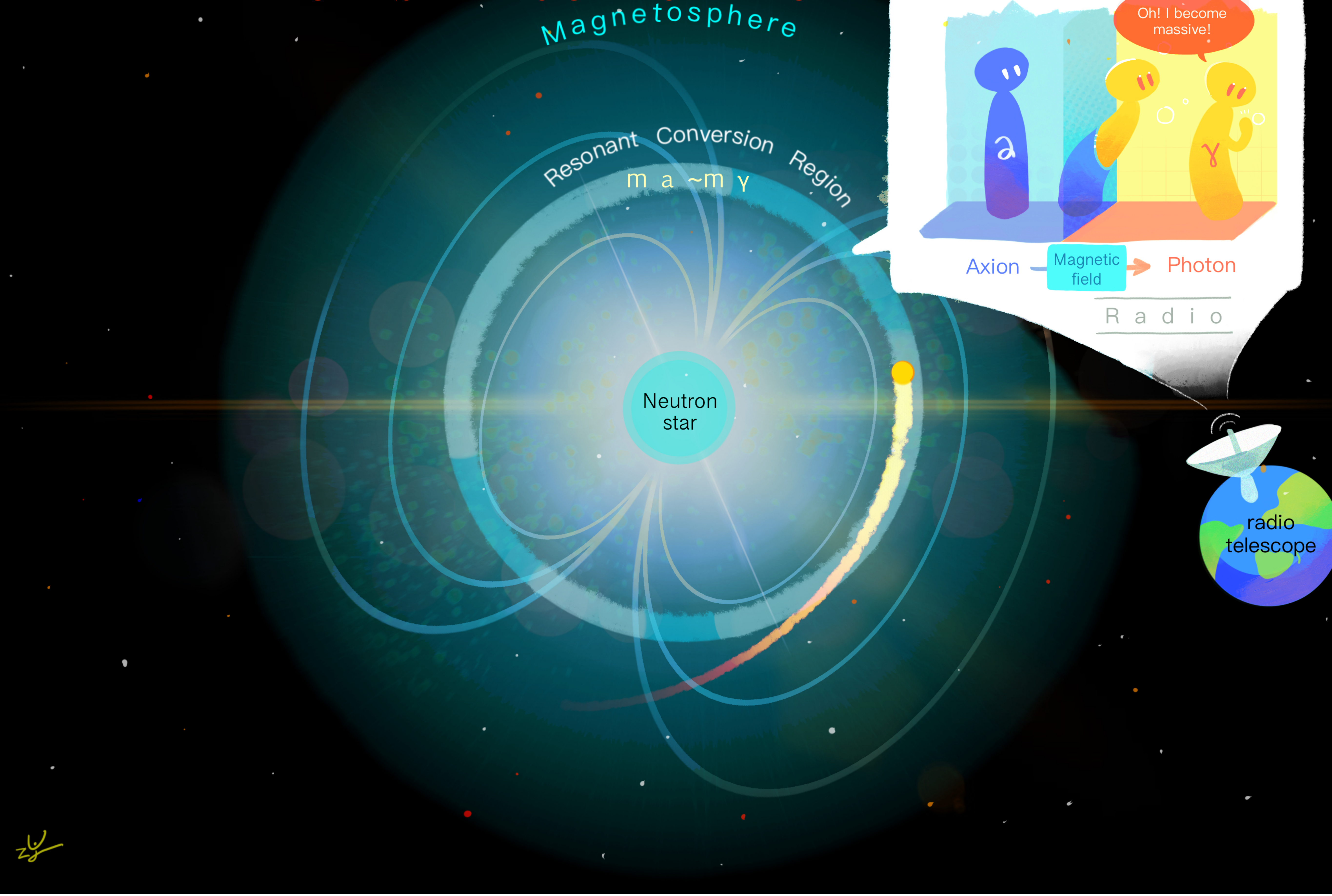

James Buckley, Bhupal Dev, Francesc Ferrer, FPH, arXiv:2004.06486

Generalisation to dark photon DM case

Raidofrequency Dark Photon Dark Matter across the Sun, **Haipeng An, FPH, Jia Liu, Wei Xue arXiv:2010.15836**

Recently, people realize light dark photon can be a promising DM candidate.
We study how to detect this dark photon DM by radio telescope, following the same idea as the axion DM case.
We can obtain the strongest constraint.

P. W. Graham, J. Mardon and S. Rajendran, Phys. Rev. D **93**, no. 10, 103520 (2016) doi:10.1103/PhysRevD.93.103520 [arXiv:1504.02102 [hep-ph]].

R. T. Co, A. Pierce, Z. Zhang and Y. Zhao, Phys. Rev. D **99**, no. 7, 075002 (2019) doi:10.1103/PhysRevD.99.075002 [arXiv:1810.07196 [hep-ph]].

P. Agrawal, N. Kitajima, M. Reece, T. Sekiguchi and F. Takahashi, arXiv:1810.07188 [hep-ph].

A. J. Long and L. T. Wang, Phys. Rev. D **99**, no. 6, 063529 (2019) doi:10.1103/PhysRevD.99.063529 [arXiv:1901.03312 [hep-ph]].

Generalisation to dark photon DM case

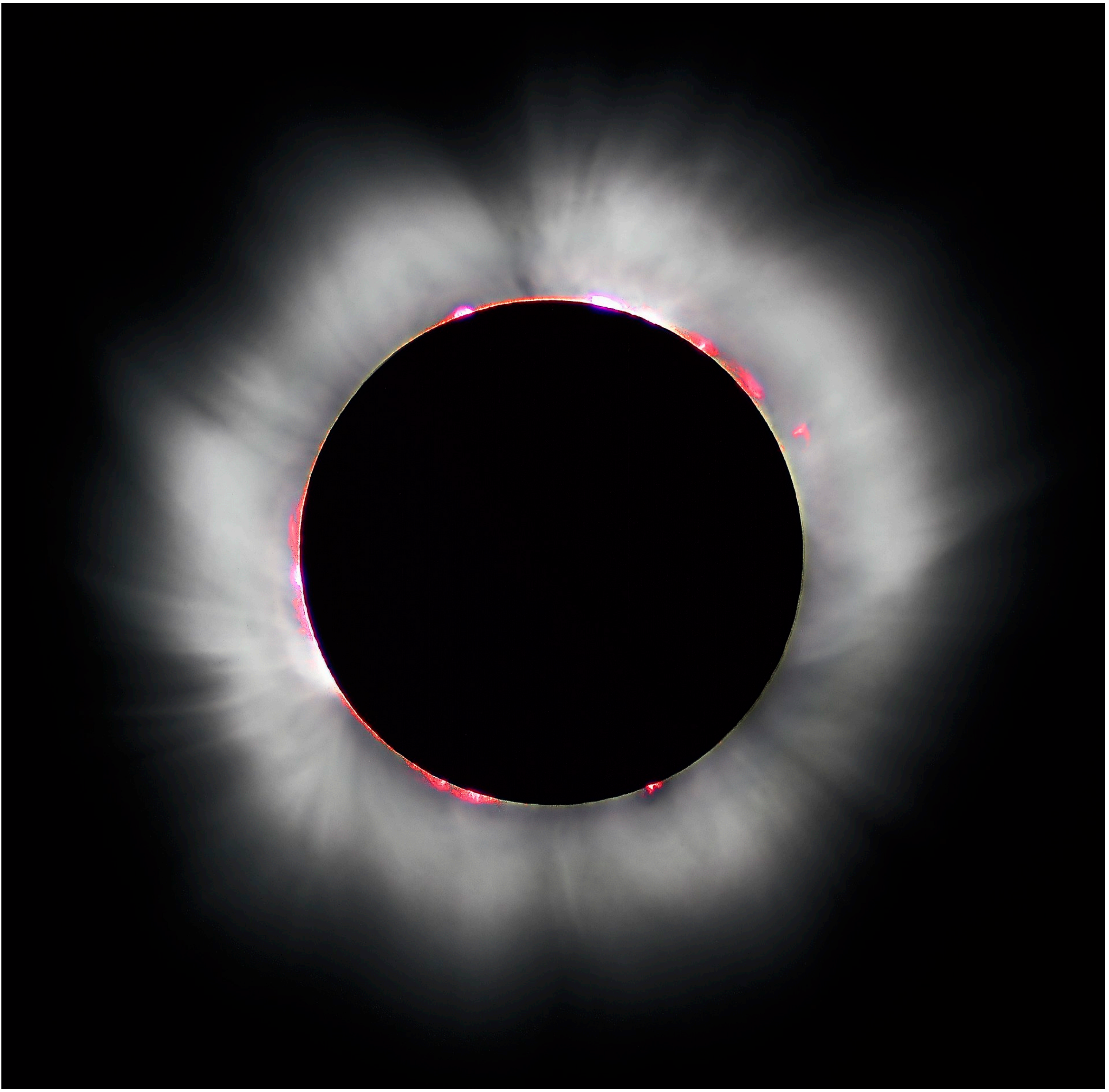

For dark photon DM, the resonant conversion could happen without magnetic Field. We can directly study the resonant conversion process in the solar corona.

Two advantages: closer and larger conversion volume.
Disadvantage: stronger background

During a total solar eclipse, the Sun's corona and prominences are visible to the naked eye.

Generalisation to dark photon DM case

Raidofrequency Dark Photon Dark Matter across the Sun, **Haipeng An, FPH, Jia Liu, Wei Xue arXiv:2010.15836**

$$\mathcal{L} = -\frac{1}{4}F'_{\mu\nu}F'^{\mu\nu} - \frac{1}{2}m_{A'}^2 A'_\mu A'^\mu - \frac{1}{2}\epsilon F_{\mu\nu}F'^{\mu\nu} \ , \qquad (1)$$

where $F_{\mu\nu}$ is the photon field strength, A' is the dark photon field, $F'^{\mu\nu}$ is the dark photon field strength, and ϵ is the kinetic mixing. With this mixing term, the dark photons can oscillate resonantly into photons in thermal plasma once the plasma frequency ω_p roughly equals $m_{A'}$. The plasma frequency for non-relativistic plasma relies on the electron density n_e,

$$\omega_p = \left(\frac{4\pi\alpha n_e}{m_e}\right)^{1/2} = \left(\frac{n_e}{7.3\times 10^8\ \text{cm}^{-3}}\right)^{1/2} \mu\text{eV} \ , \qquad (2)$$

Generalisation to dark photon DM case

Raidofrequency Dark Photon Dark Matter across the Sun, **Haipeng An, FPH, Jia Liu, Wei Xue arXiv:2010.15836**

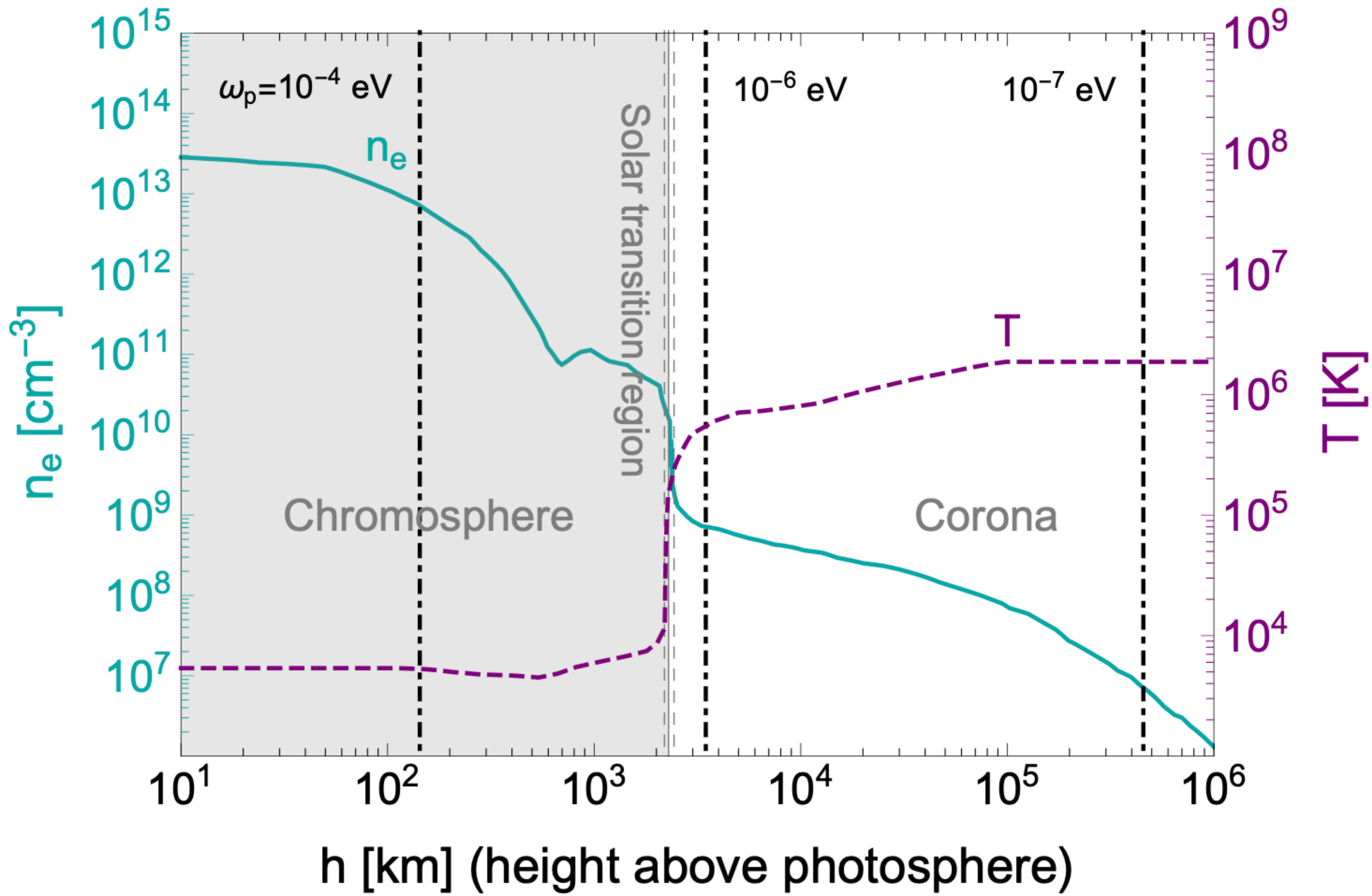

Resonant production

Raidofrequency Dark Photon Dark Matter across the Sun, **Haipeng An, FPH, Jia Liu, Wei Xue arXiv:2010.15836**

$$P_{A'\to\gamma}(v_r) = \frac{1}{3}\int \frac{\mathrm{d}t}{2\omega}\frac{\mathrm{d}^3p}{(2\pi)^3 2\omega}(2\pi)^4\delta^4\left(p^\mu_{A'} - p^\mu_\gamma\right)\sum_{\mathrm{pol}}|\mathcal{M}|^2$$

$$= \frac{2}{3}\times\pi\,\epsilon^2\, m_{A'}\, v_r^{-1}\left|\frac{\partial\ln\omega_p^2(r)}{\partial r}\right|^{-1}_{\omega_p(r)=m_{A'}}, \quad (3)$$

$$\frac{d\mathcal{P}}{d\Omega} \approx 2\times\frac{1}{4\pi}\rho_{\mathrm{DM}}\, v_0\int_0^b \mathrm{d}z\, 2\pi z\, P_{A'\to\gamma}(v_r)$$

$$= P_{A'\to\gamma}(v_0)\,\rho_{\mathrm{DM}}\, v(r_c)\; r_c^2\,,$$

Propagation effects

Raidofrequency Dark Photon Dark Matter across the Sun, **Haipeng An, FPH, Jia Liu, Wei Xue arXiv:2010.15836**

It turns out that the dominant absorption process is the inverse bremsstrahlung process.

$$\Gamma_{\rm inv} \approx \frac{8\pi n_e n_N \alpha^3}{3\omega^3 m_e^2}\left(\frac{2\pi m_e}{T}\right)^{1/2}\log\left(\frac{2T^2}{\omega_p^2}\right)\left(1-e^{-\omega/T}\right)$$

$$\Gamma_{\rm Com} = \frac{8\pi\alpha^2}{3m_e^2} n_e .$$

$$P_s \equiv e^{-\int \Gamma_{\rm att} dt} \simeq \exp\left(-\int_{r_c}^{r_{\rm max}} \Gamma_{\rm att}\, dr/v_r\right)$$

Sensitivity of radio telescope

The minimum detectable flux density of a radio telescope is

$$S_{\rm min} = \frac{\rm SEFD}{\eta_s \sqrt{n_{\rm pol}\, \mathcal{B}\, t_{\rm obs}}}$$

$${\rm SEFD} = 2k_B \frac{T_{\rm sys} + T_{\odot}^{\rm nos}}{A_{\rm eff}}$$

Name	f [MHz]	$B_{\rm res}$ [kHz]	$\langle T_{\rm sys} \rangle$ [K]	$\langle A_{\rm eff} \rangle$ [m^2]
SKA1-Low	(50, 350)	1	680	2.2×10^5
SKA1-Mid B1	(350, 1050)	3.9	28	2.7×10^4
SKA1-Mid B2	(950, 1760)	3.9	20	3.5×10^4
LOFAR	(10, 80)	195	28,110	1,830
LOFAR	(120, 240)	195	1,770	1,530

The sensitivity reach

Raidofrequency Dark Photon Dark Matter across the Sun, **Haipeng An, FPH, Jia Liu, Wei Xue arXiv:2010.15836 under review in Phy. Rev. Let**

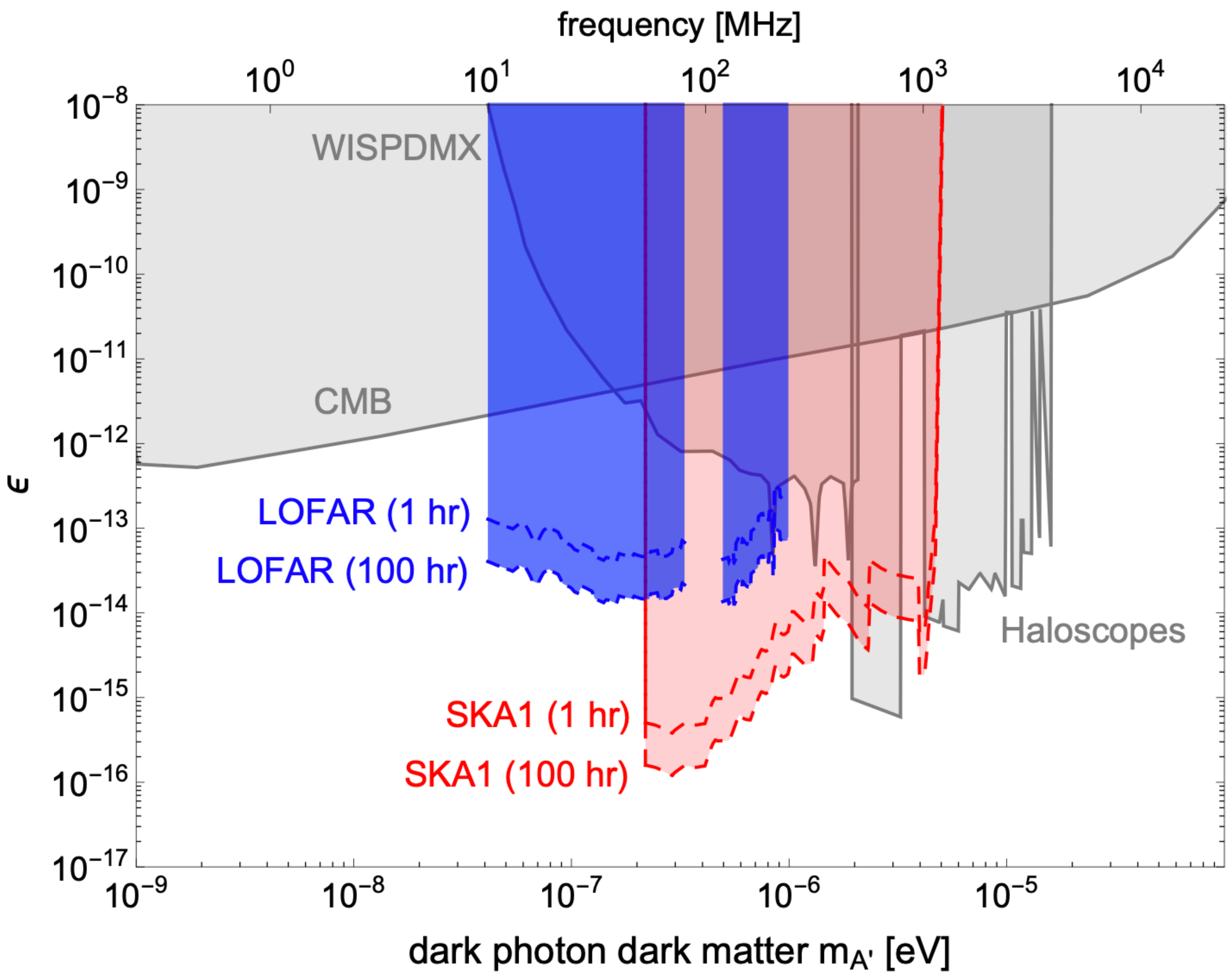

II. How can we use gravitational waves to explore dark matter?

➢The observation of GW by LIGO has initiated a new era of exploring DM by GW.

➢ DM can trigger first-order phase transition in the early universe, which can leads to detectable gravitational wave signals.

➢New DM production scenario filtered by the bubbles of the first-order phase transition in the early universe

Hearing the signal of dark sectors with gravitational wave detectors
J.Jaeckel, V. V. Khoze, M. Spannowsky, Phys.Rev. D94 (2016) no.10, 103519

Yan Wang,Chong Sheng Li, and **FPH**, arXiv:2012.03920
FPH, Eibun Senaha Phys.Rev. D100 (2019) no.3, 03501
FPH PoS ICHEP2018 (2019) 397
FPH, Chong Sheng Li Phys.Rev. D96 (2017) no.9, 095028
FPH, Jiang-Hao Yu Phys.Rev. D98 (2018) no.9, 095022
FPH, Xinmin Zhang, Phys.Lett. B788 (2019) 288-29

What is gravitational wave?

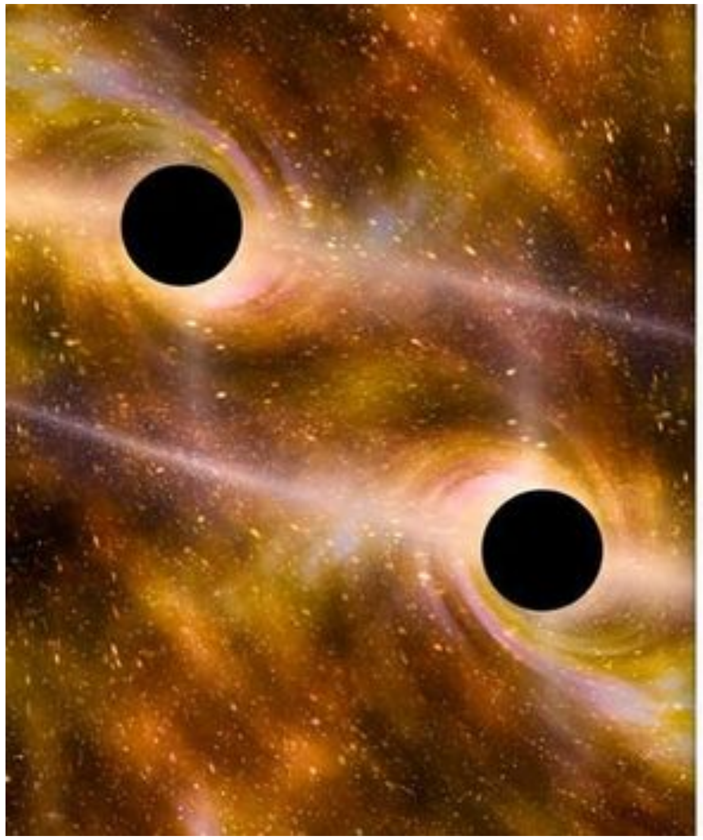

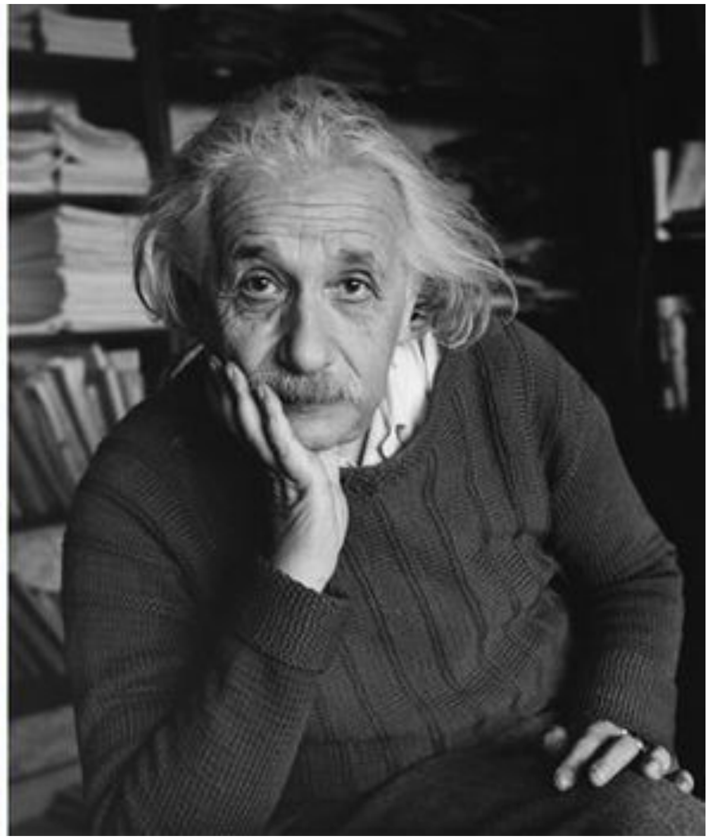

General relativity and
Warped space time

$$R_{\mu\nu} - \frac{1}{2} R\, g_{\mu\nu} + \Lambda\, g_{\mu\nu} = \frac{8\pi G}{c^4} T_{\mu\nu}$$

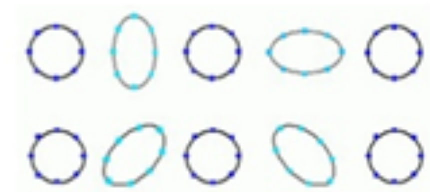

$$h_{ij} \simeq \frac{2G}{c^4 r} \ddot{Q}_{ij}^{TT}(t - r/c)$$

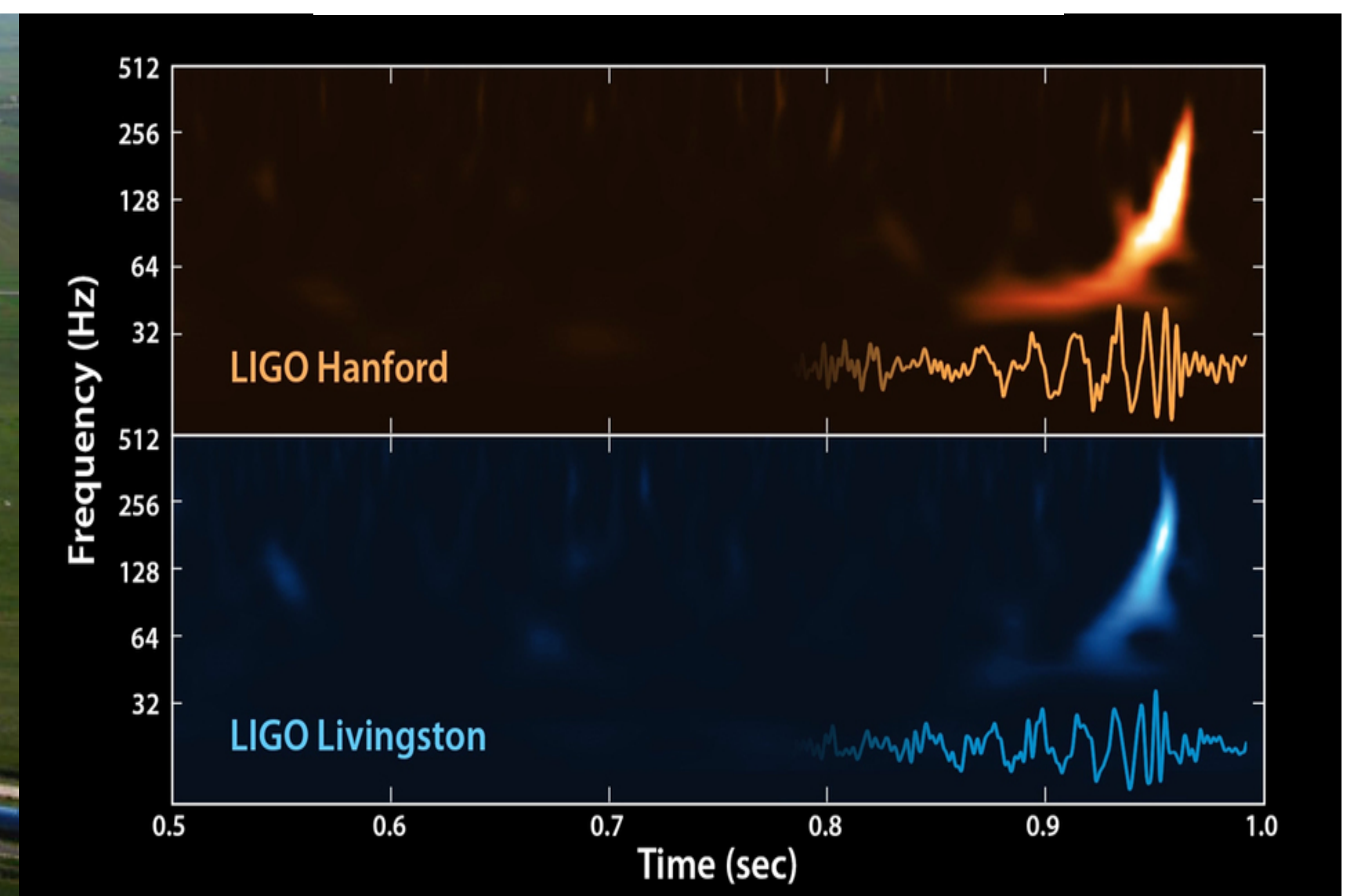

Phase transition GW in a nutshell

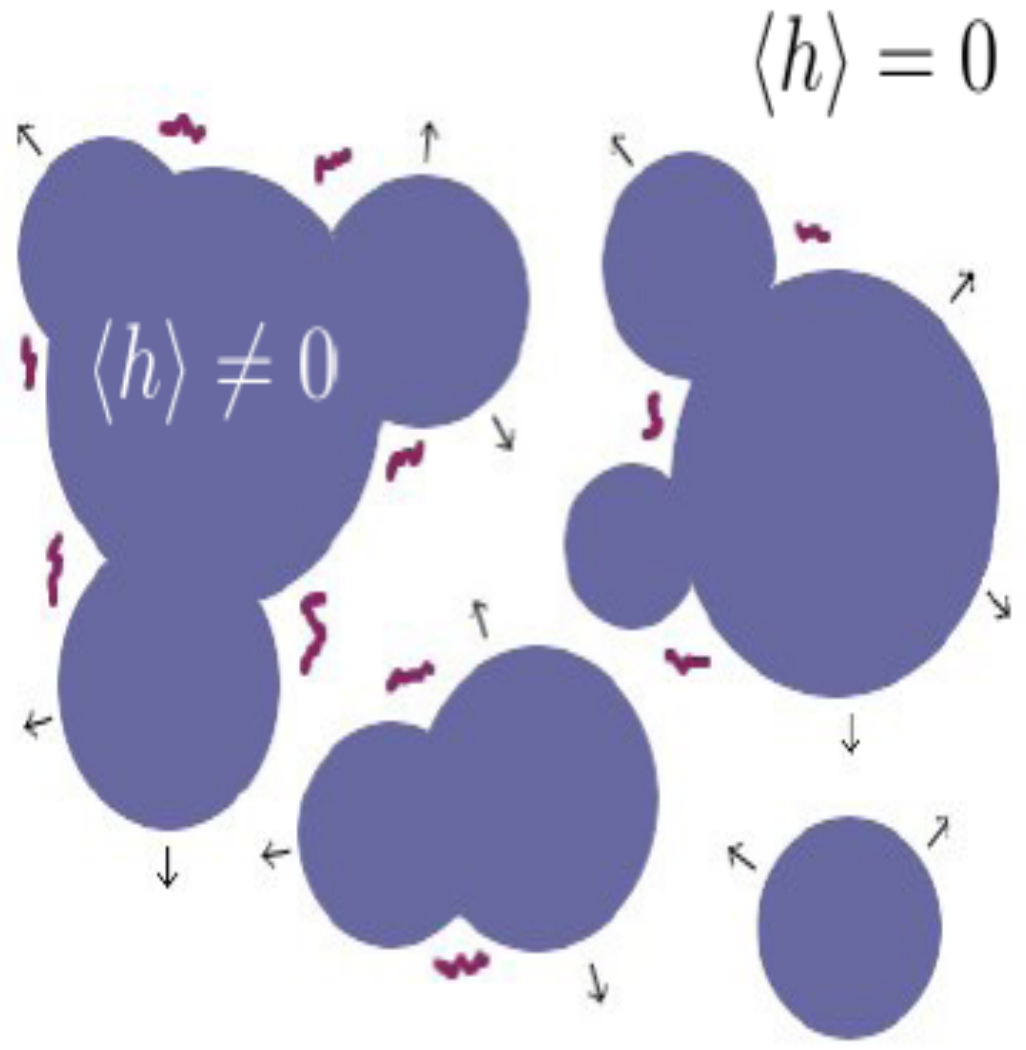

Strong First-order phase transition (SFOPT) can drive the plasma of the early universe out of thermal equilibrium, and bubbles nucleate during it, which will produce GW.

E. Witten, Phys. Rev. D 30, 272 (1984)
C. J. Hogan, Phys. Lett. B 133, 172 (1983);
M. Kamionkowski, A. Kosowsky and M. S. Turner, Phys. Rev. D 49, 2837 (1994))

EW phase transition GW becomes more interesting and realistic after the discovery of Higgs by LHC and GW by LIGO.

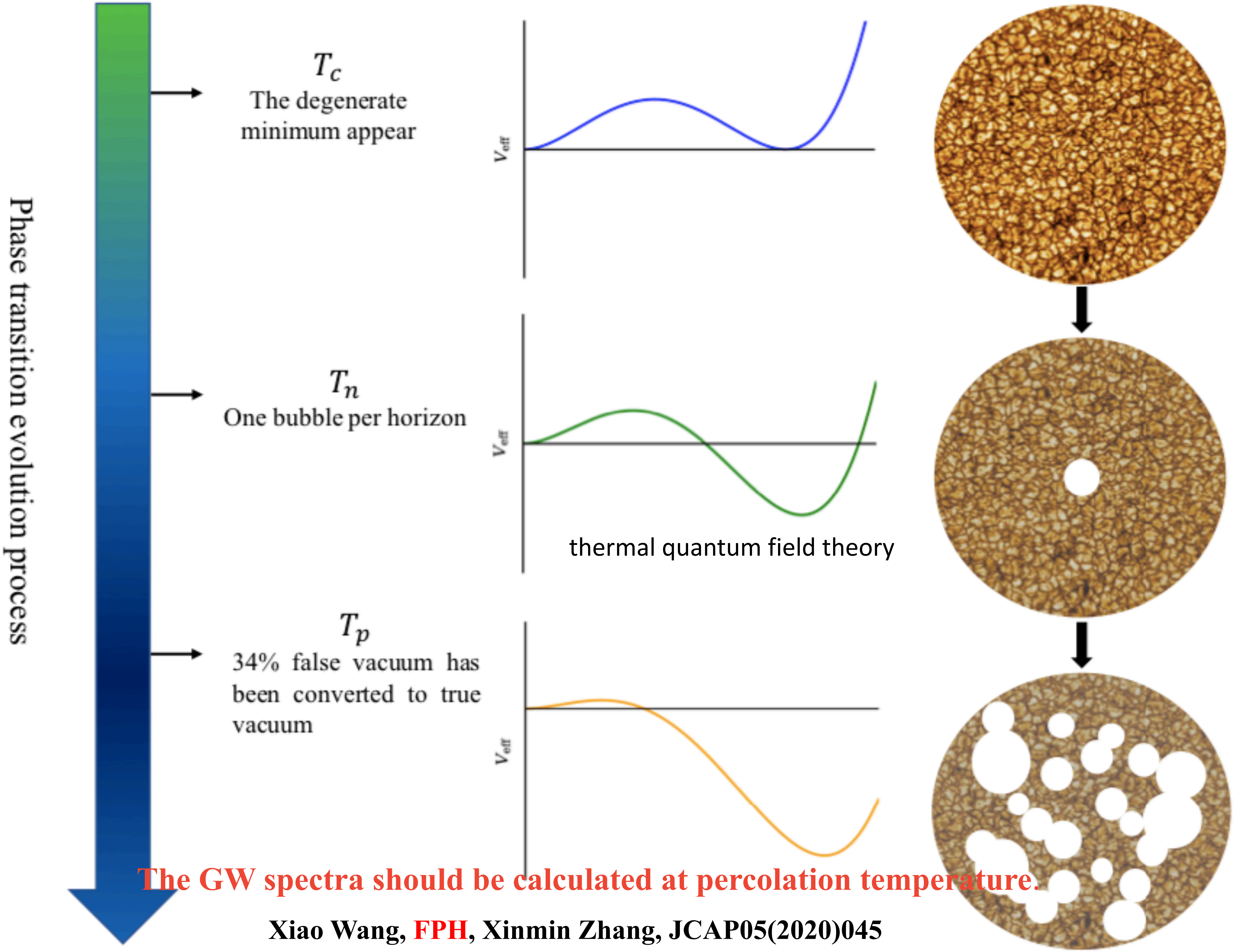
Phase transition evolution process
T_c
The degenerate minimum appear
V_{eff}
T_n
One bubble per horizon
V_{eff}
thermal quantum field theory
T_p
34% false vacuum has been converted to true vacuum
V_{eff}
The GW spectra should be calculated at percolation temperature.
Xiao Wang, FPH, Xinmin Zhang, JCAP05(2020)045

α quantifies the strength of SFOPT

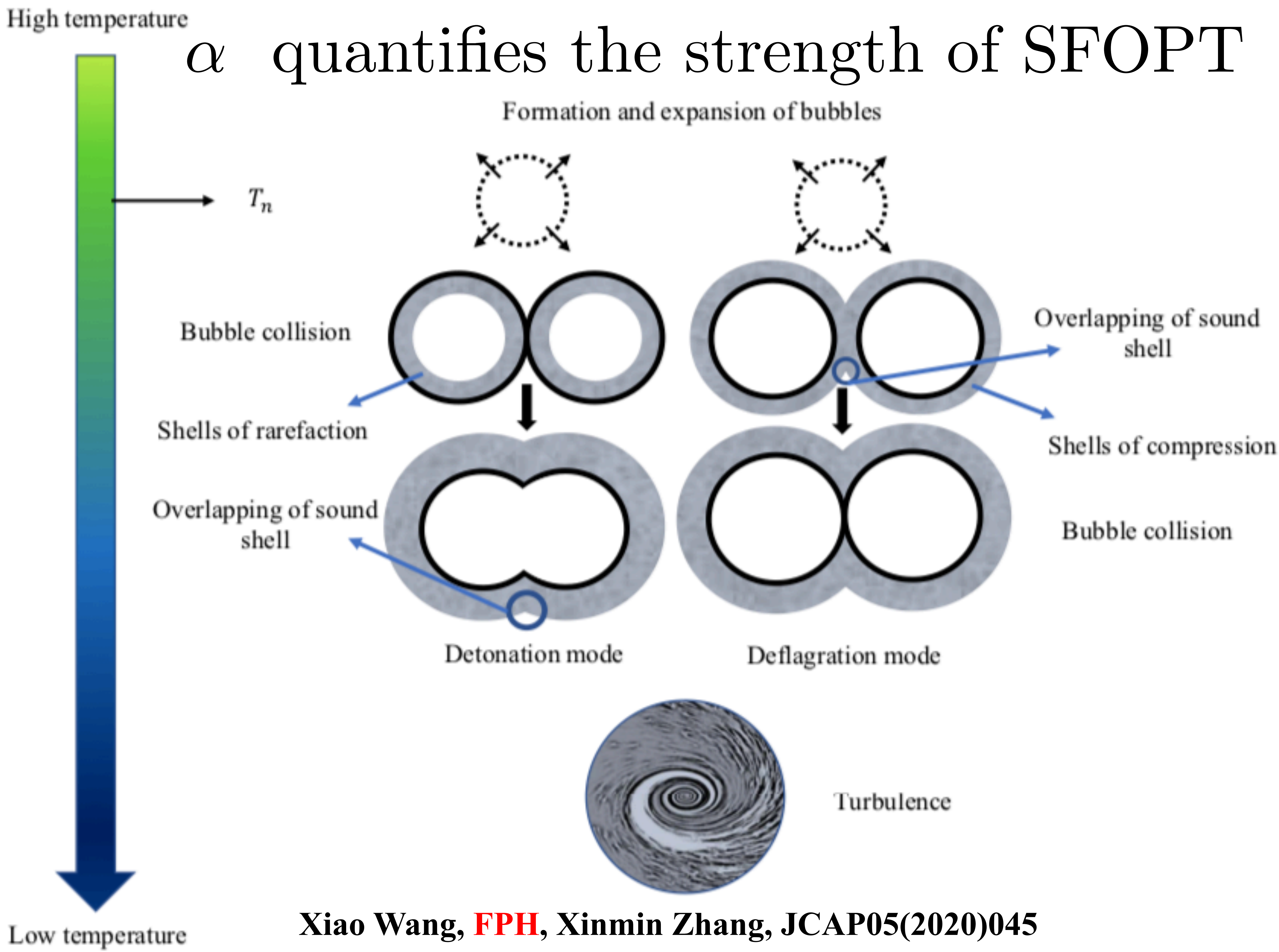

Xiao Wang, FPH, Xinmin Zhang, JCAP05(2020)045

GW signals from SFOPT

Bubble collisions

$$h^2\Omega_{\rm co}(f) \simeq 1.67\times 10^{-5}(\frac{H_*R_*}{(8\pi)^{1/3}})^2\left(\frac{\kappa_\phi\alpha}{1+\alpha}\right)^2\left(\frac{100}{g_\star}\right)^{1/3}\frac{0.11v_b}{0.42+v_b^2}\frac{3.8(f/f_{\rm co})^{2.8}}{1+2.8(f/f_{\rm co})^{3.8}}$$

Turbulence

$$h^2\Omega_{\rm turb}(f) \simeq 1.14\times 10^{-4}H_*R_*\left(\frac{\kappa_{\rm turb}\alpha}{1+\alpha}\right)^{3/2}\left(\frac{100}{g_*}\right)^{1/3}\frac{(f/f_{\rm turb})^3}{(1+f/f_{\rm turb})^{11/3}(1+8\pi f/H_*)}$$

Sound wave

$$h^2\Omega_{\rm sw}(f) \simeq 1.64\times 10^{-6}(H_*\tau_{\rm sw})(H_*R_*)\left(\frac{\kappa_v\alpha}{1+\alpha}\right)^2\left(\frac{100}{g_*}\right)^{1/3}(f/f_{\rm sw})^3\left(\frac{7}{4+3(f/f_{\rm sw})^2}\right)^{7/2}$$

E. Witten, Phys. Rev. D 30, 272 (1984)
C. J. Hogan, Phys. Lett. B 133, 172 (1983);
M. Kamionkowski, A. Kosowsky and M. S. Turner, Phys. Rev. D 49, 2837 (1994))Mark Hindmarsh, *et al.*, PRL 112, 041301 (2014); Lots of unlisted papers.

Inert Doublet DM Models

The tree-level potential to describe the inert doublet DM model is given by

$$
\begin{aligned}
V_0 \;=\;& M_D^2 D^\dagger D + \lambda_D (D^\dagger D)^2 + \lambda_3 \Phi^\dagger \Phi D^\dagger D \\
+\;& \lambda_4 |\Phi^\dagger D|^2 + (\lambda_5/2)[(\Phi^\dagger D)^2 + h.c.],
\end{aligned}
$$

provide natural DM candidate

provide strong first-order phase transition（FOPT） and phase transition GW

FPH, Jiang-hao Yu, PHY. REV. D 98, 095022 (2018)

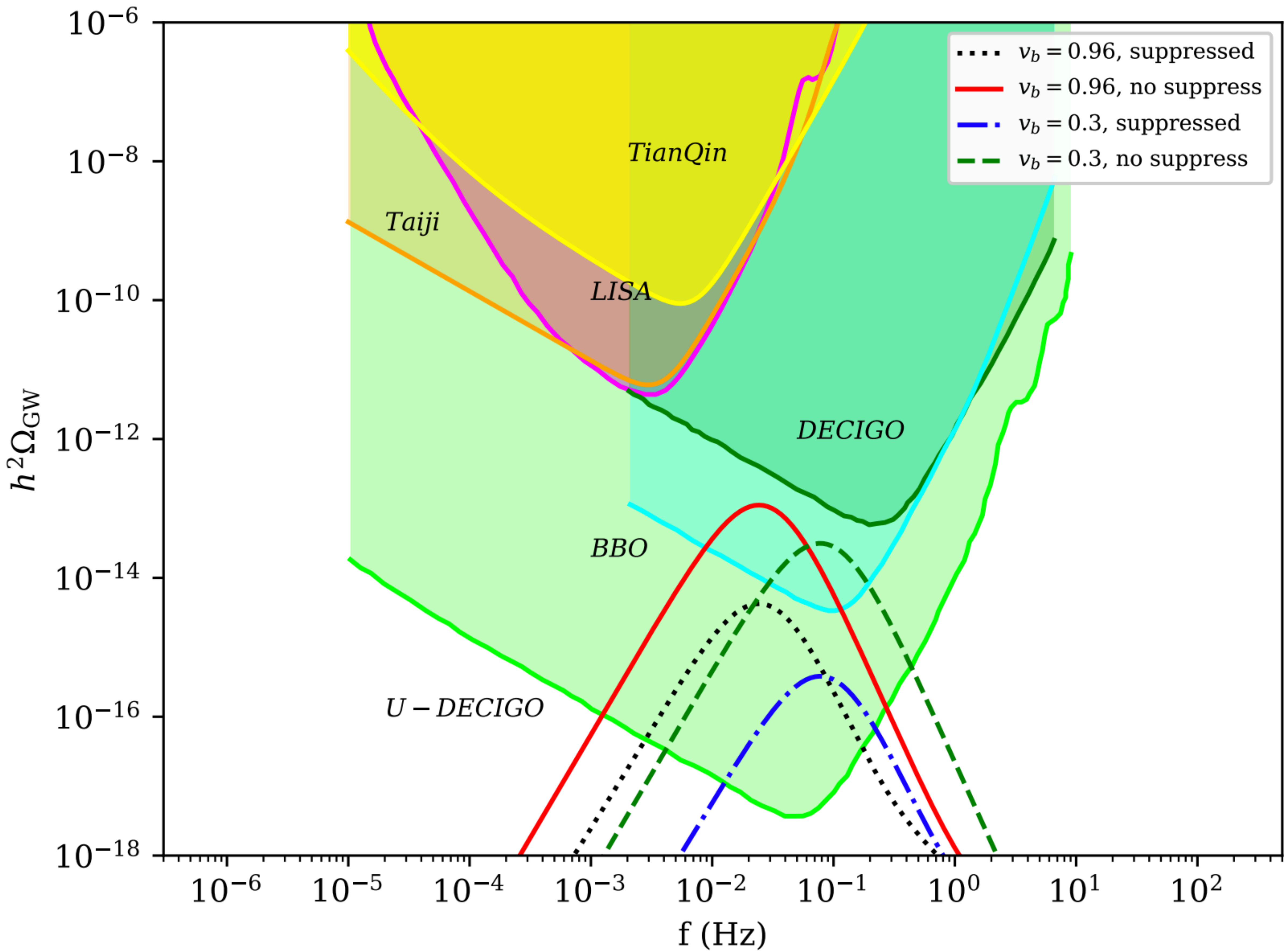

Yan Wang,Chong Sheng Li, and **FPH**, arXiv:2012.03920

The mixed singlet-doublet DM model

The tree-level potential to describe the mixed singlet-doublet DM model is given by

$$V_0 = \frac{1}{2}M_S^2 S^2 + M_D^2 H_2^\dagger H_2 + \frac{1}{2}\lambda_S S^2 |\Phi|^2 + \lambda_3 \Phi^\dagger \Phi H_2^\dagger H_2 + \lambda_4 |\Phi^\dagger H_2|^2 + \frac{\lambda_5}{2}[(\Phi^\dagger H_2)^2 + \mathrm{H.c.}] + A[S\Phi H_2^\dagger + \mathrm{H.c.}].$$

provide natural DM candidate

provide strong first-order phase transition and phase transition GW

FPH, Jiang-hao Yu, PHY. REV. D 98, 095022 (2018)

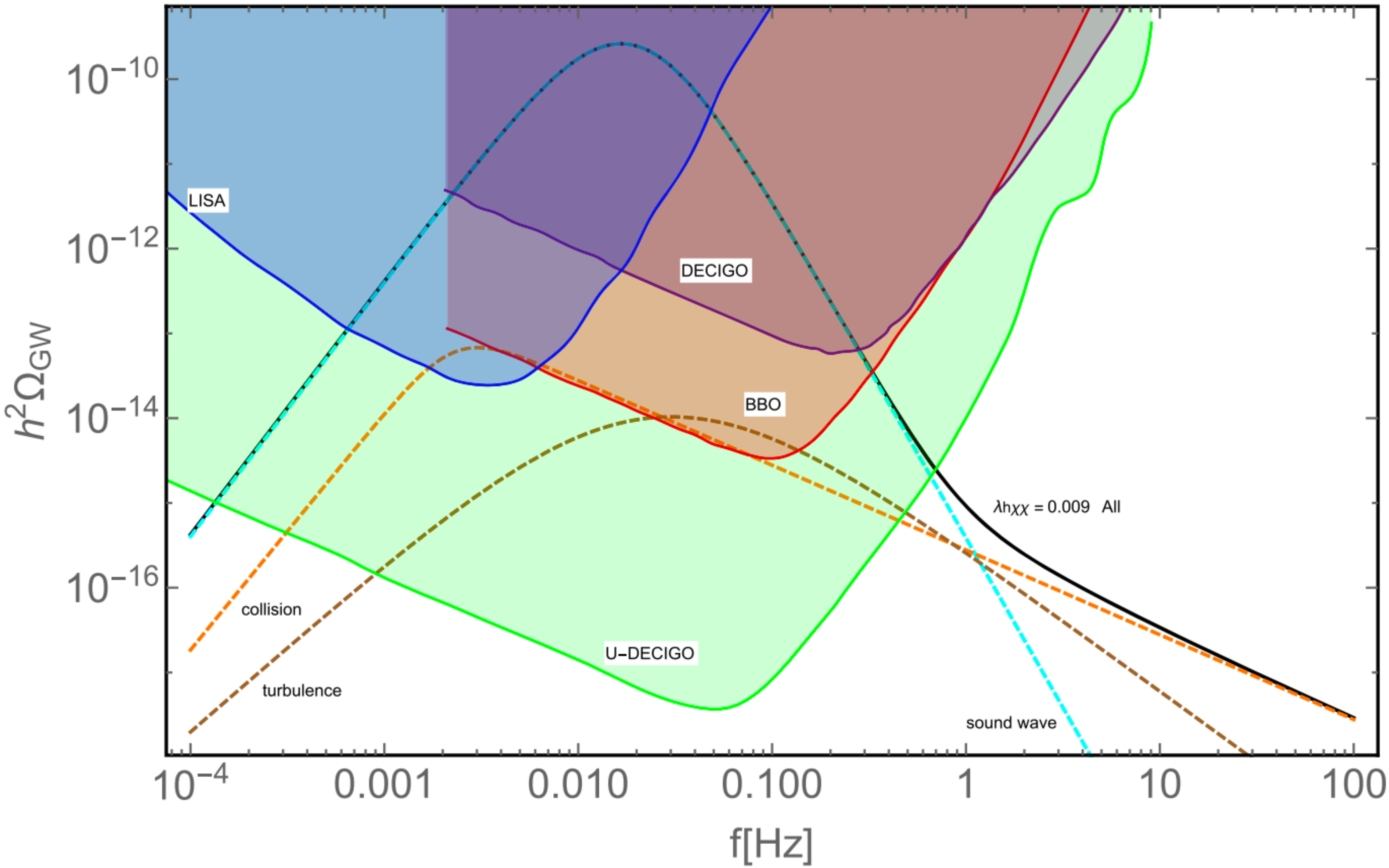

$h^2\Omega_{GW}$
10^{-10}
10^{-12}
10^{-14}
10^{-16}
LISA
DECIGO
BBO
U-DECIGO
collision
turbulence
sound wave
$\lambda h\chi\chi = 0.009$ All
10^{-4}
0.001
0.010
0.100
1
10
100
f[Hz]

Heavy DM formed by SFOPT

The cosmic phase transition with Q-balls production can explain baryogenesis and DM simultaneously, where constraints on DM mass and reverse dilution are significantly relaxed. We study how to probe this scenario by GW signals and collider signals at QCD NLO.

FPH, Chong Sheng Li, Phys.Rev. D96 (2017) no.9, 095028

Many mechanisms to simultaneously solve the baryogenesis and DM puzzles usually have two strong constraints.

B. Shuve, C. Tamarit, JHEP 1710 (2017) 122

In usual asymmetry dark matter models, $n_{DM} \sim n_B, \ \rho_{DM} \approx 5\rho_B$

→ $$m_{DM} \approx 5m_p \approx 5GeV$$

SFOPT naturally correlates DM, baryogenesis, particle collider and GW signals.

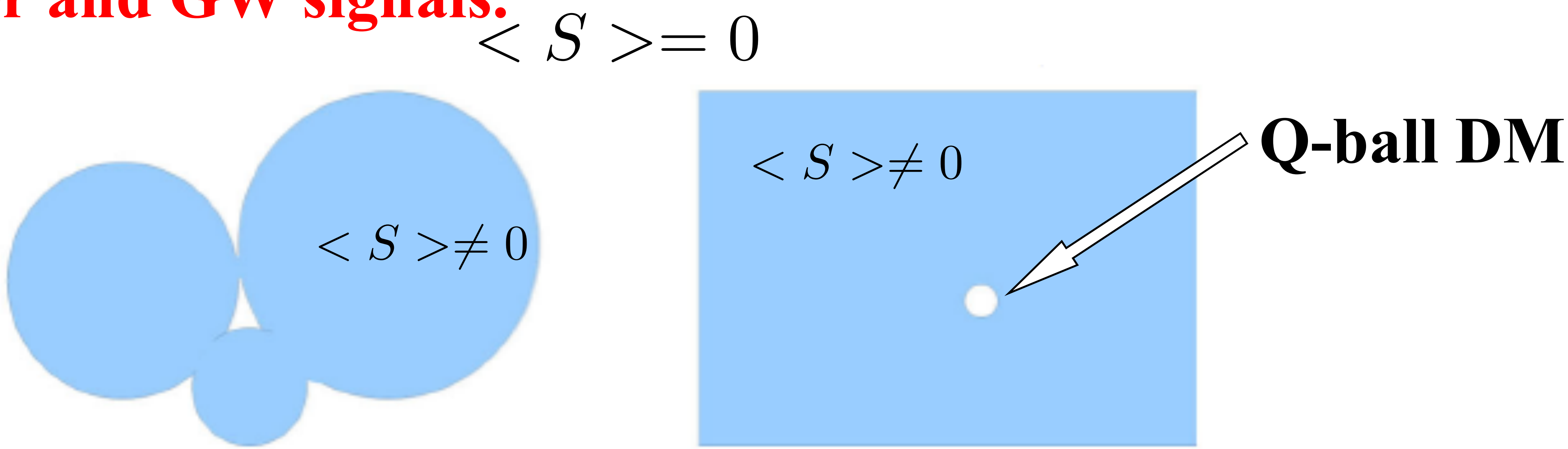

And with the bubble expansion, the symmetric phase eventually shrinks to very small size objects and become the so-called Q-balls as DM candidates.

$$
\begin{aligned}
\mathcal{L} = & \frac{1}{2}(\partial_\mu S)^2 - U(S) + (\partial_\mu \chi)^*(\partial_\mu \chi) - k_1^2 S^2 \chi^* \chi \\
& - \sum_i \frac{h_i^2}{2} S^2 \phi_i^2 + \sum_i \frac{1}{2}(\partial_\mu \phi_i)^2 \\
& - \sum_{a=1,2} \frac{\lambda_a^{ijk}}{\Lambda^2} \bar{X}_a P_R D_i \bar{U}_j^C P_R D_k + \frac{\zeta_a}{\Lambda} \bar{X}_a Y^C \chi \chi^* \\
& + \text{H.c.}
\end{aligned}
$$

Final conditions to produce the observed baryon asymmetry and DM density: FPH, C.S. Li, Phys.Rev. D96 (2017) no.9, 09502

$$\rho_{\rm DM}^4 v_b^{3/4} = 73.5(2\eta_B s_0)^3 \lambda_S \sigma^4 \Gamma^{3/4}$$

TABLE I. The benchmark sets after considering the combined constraints for producing the observed DM density and BAU with $v_b = 0.3$.

Benchmark sets	λ_S	e	c	T_c [TeV]	$\frac{\sigma}{T_C}$
I	0.008	0.754	1	15.9	5
II	0.0016	0.151	1	6.6	5

Extension work for the gauged Q-balls is working in progress with Prof. P. Ko

The predicted GW spectrum for benchmark points with $v_b = 0.3$. Figure(a), (b), (c) represents the GW spectrum from bubble collision, sound waves and turbulence, respectively, which may be detected by future LIGO-like experiments, Einstein telescope or cosmic explorer.

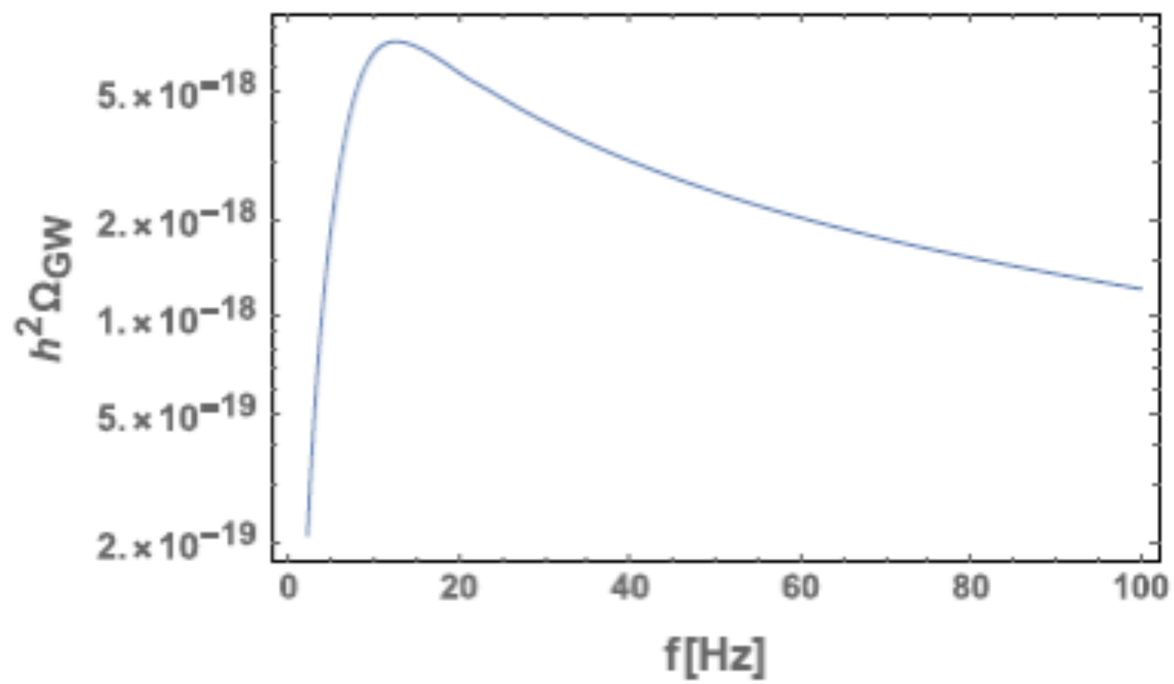

(a)

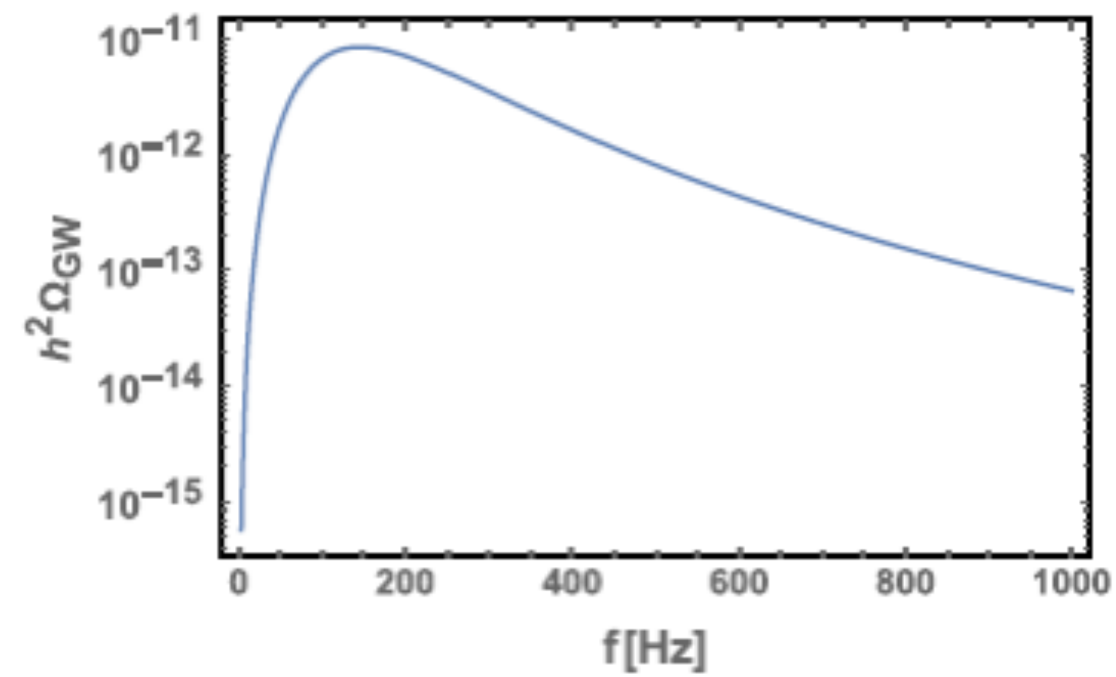

(b)

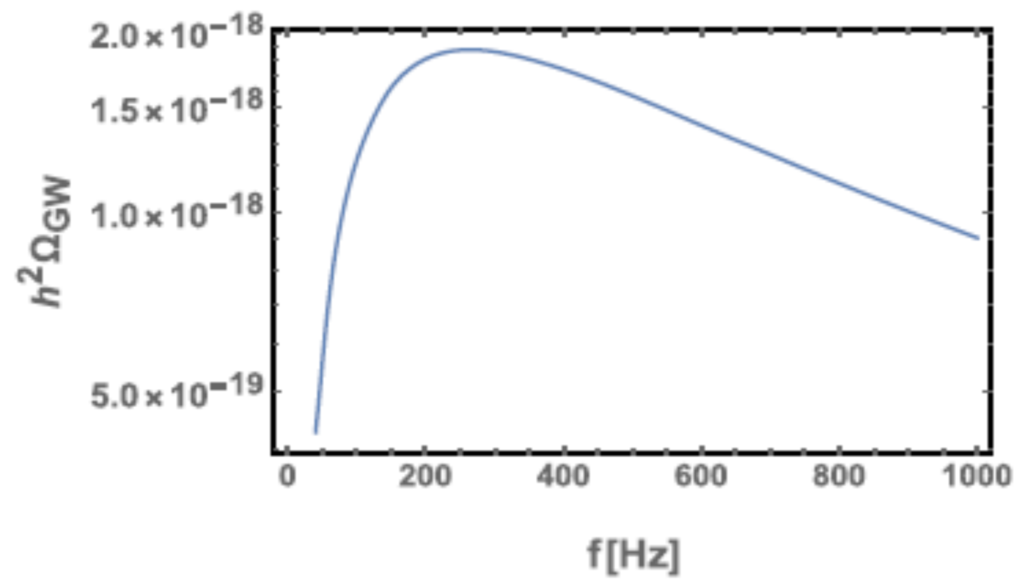

(c)

Collider phenomenology

There are many types of combinations for the up-type quark and down-type quark, which result in abundant collider phenomenology at the LHC.

The dominant decay channel behaves as the missing energy in the detector. So the interactions can be explored by performing mono-jet and mono-top analysis at the LHC.

Because the LHC is a proton-proton collider with high precision, the QCD NLO predictions for these processes are necessary in order to obtain reliable results.

QCD NLO prediction at the LHC

We perform QCD the next-leading-order (NLO) predictions for these two cases and discuss the discovery potential at the LHC.

The Key point for QCD NLO calculation is Infrared divergence

Origin of singular contributions: soft and collinear emission

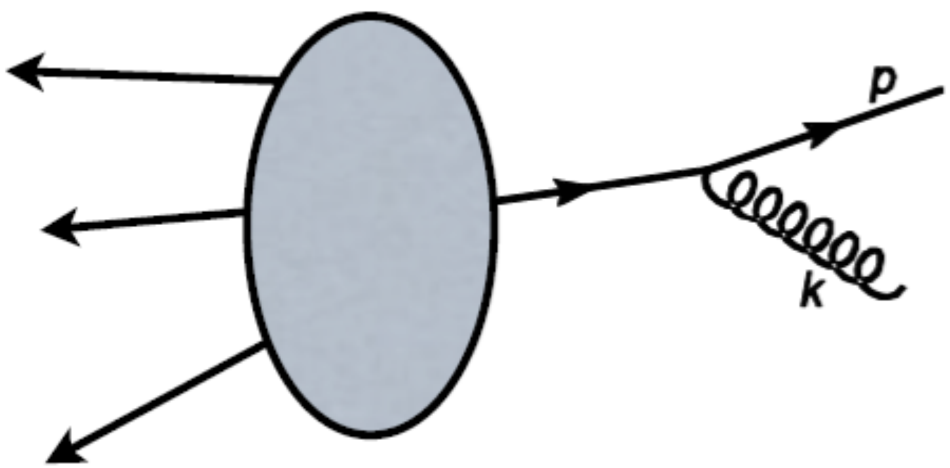

$$\frac{1}{(p+k)^2} = \frac{1}{2\,p\cdot k} = \frac{1}{2E_q E_g(1-\cos\theta_{qg})}$$

soft — collinear

Tricks for QCD NLO calculations:
Two cutoff phase space slicing method (δs,δc)
or dipole subtraction

Mono-jet analysis at QCD NLO

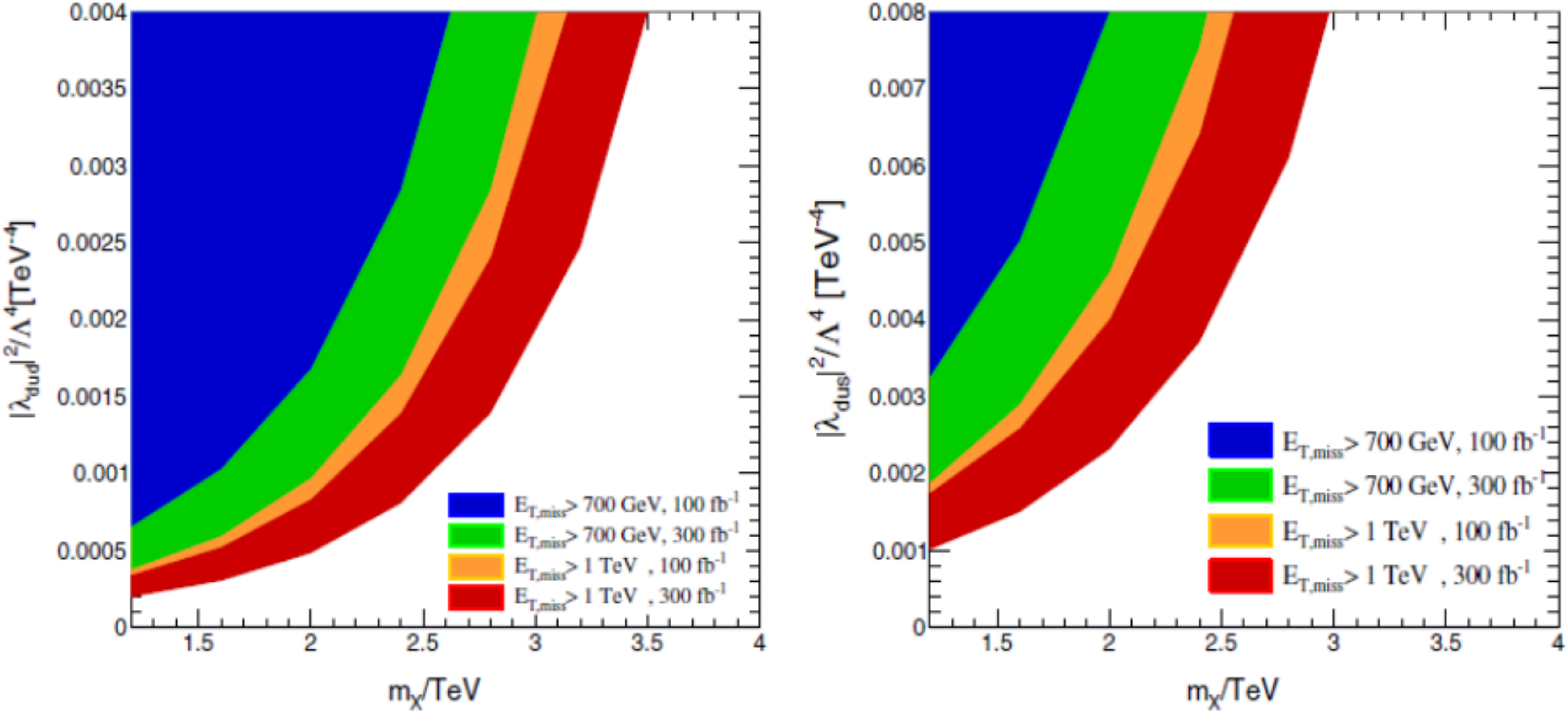

Constraints on coupling λ_{ijk} and mass m_X by monojet measurements at the 13 TeV LHC.

Mono-top analysis at QCD NLO

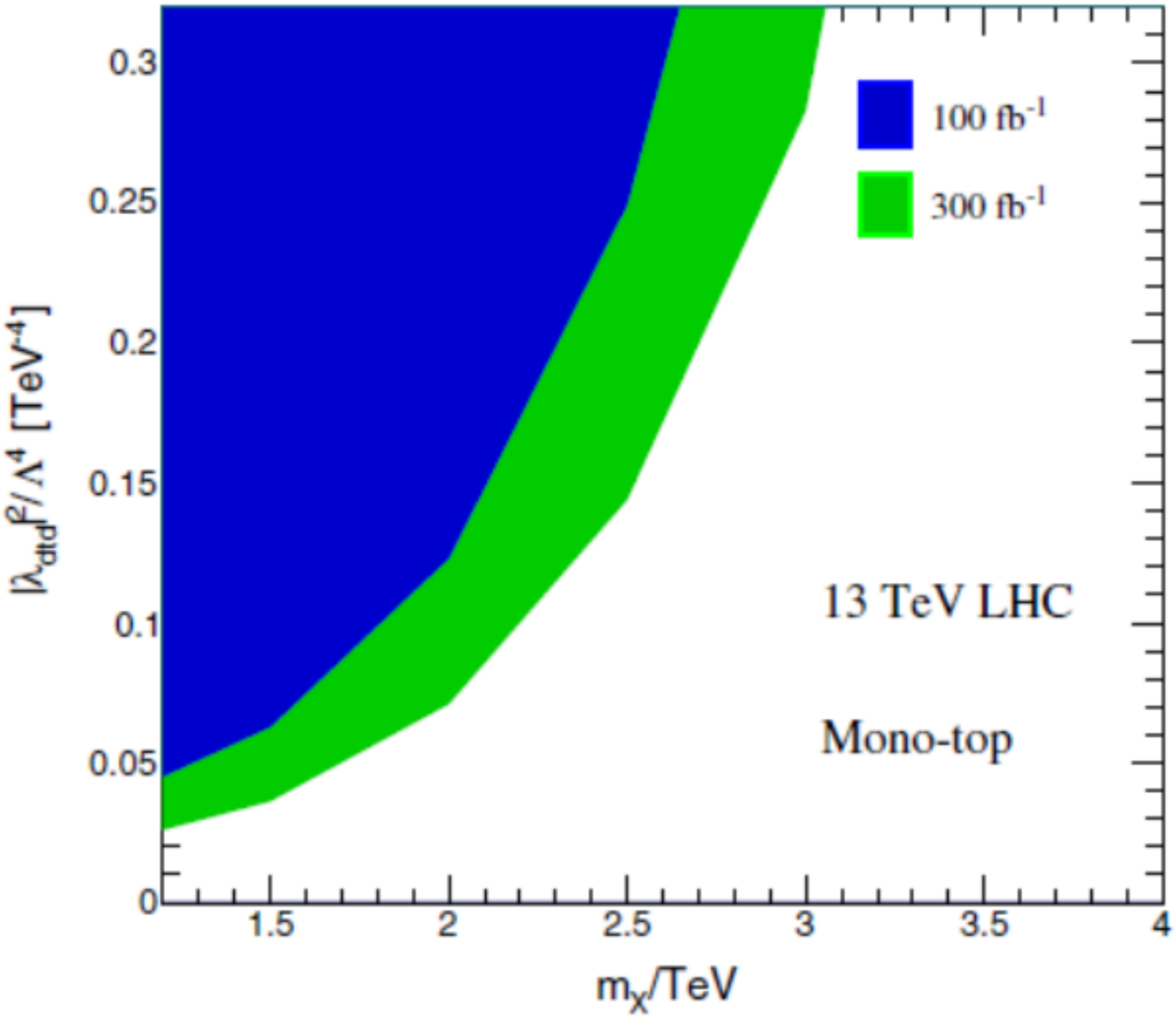

FPH, C.S. Li, **Phys.Rev. D96 (2017) no.9, 095028**

FPH, Chong Sheng Li, Phys.Rev. D96 (2017) no.9, 095028, cited by 25

In the recent two years, this dynamical DM formed by phase transition has became a new idea and attracted more and more attentions. Namely , bubble in SFOPT can be the "filters" to packet your needed heavy DM.

arXiv:1912.04238,Dongjin Chway, Tae Hyun Jung, Chang Sub Shin
arXiv:1912.0283, Michael J. Baker,Joachim Kopp,and Andrew J. Long
arXiv:2012.15113,Wei Chao,1 Xiu-Fei Li,1 Lei Wang
arXiv:2103.09827, Pouya Asadi , Eric David Kramer, Eric Kuflik, Gregory W. Ridgway, Tracy R. Slatyer, Juri Smirnov
arXiv:2103.09822, Pouya Asadi , Eric David Kramer, Eric Kuflik, Gregory W. Ridgway, Tracy R. Slatyer, Juri Smirnov

More general cases for DM

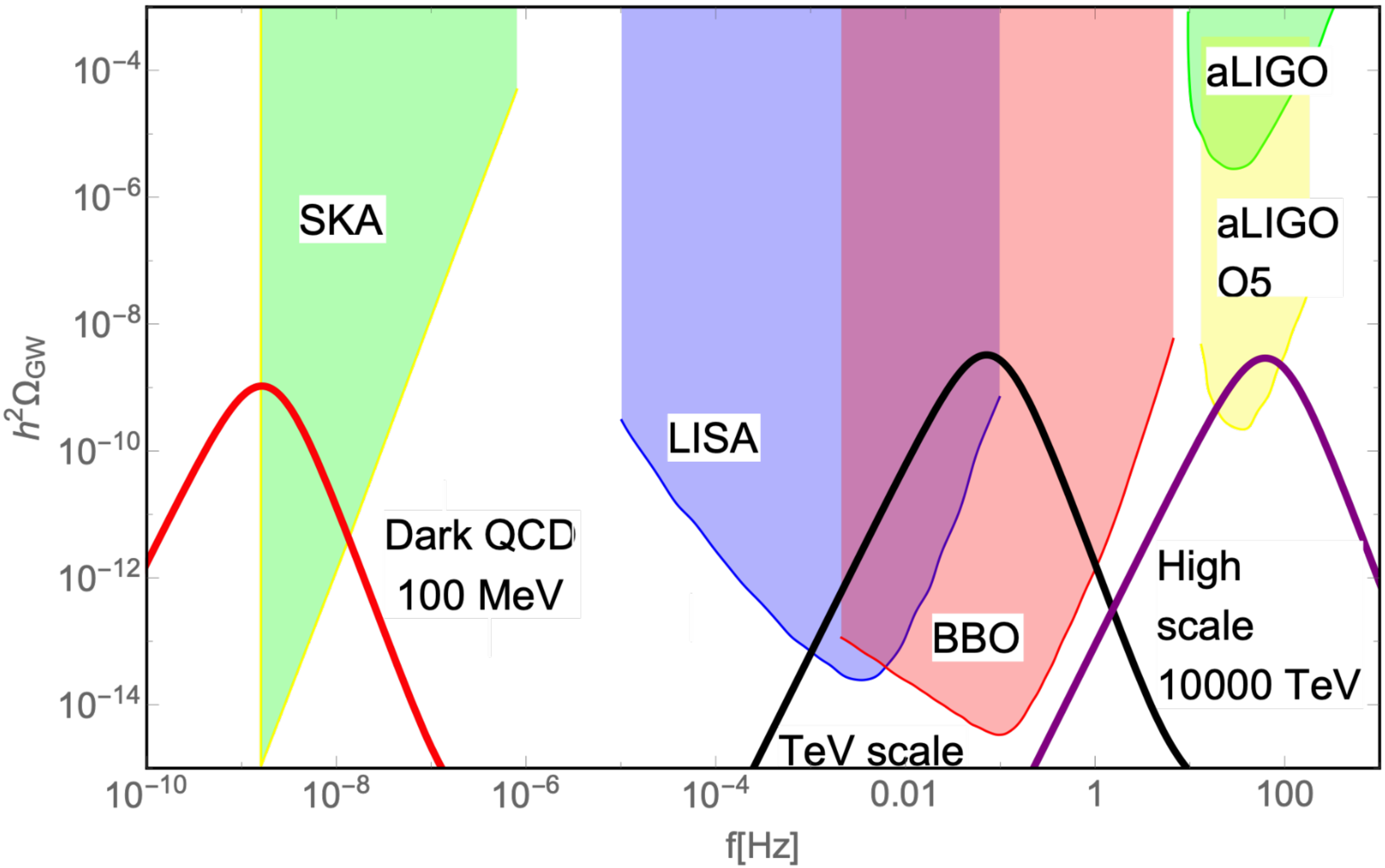

Schematic phase transition GW spectra for SKA-like and LISA-like experiments to explore DM and baryogenesis

FPH, Xinmin Zhang, Physics Letters B 788 (2019) 288-294

Conclusion

Radio signals and gravitational wave signals can provide new indirect approaches to explore the nature of dark matter.

Thanks for your attention!

Comments and collaborations are welcome!